TECHNICAL UNIVERSITY OF CIVIL ENGINEERING BUCHAREST

Faculty of Railways, Roads and Bridges

PhD Thesis

Summary

Studies on the calculation methods of deep excavations

PhD Student
eng. Cătălin CĂPRARU

PhD Supervisor
Professor PhD Anton CHIRICĂ

BUCHAREST
2012

TECHNICAL UNIVERSITY OF CIVIL ENGINEERING BUCHAREST

Faculty of Railways, Roads and Bridges

The holder of this PhD thesis has benefited during his entire doctoral study period a scholarship awarded by the strategic project ***„Support for PhD students in Built Environment Engineering”****, whose beneficiary is TUCEB, code OPHRD/88/1.5/S/57351. The project developed within the Operational Program for Human Resources Development, financed by the European Structural Funds, the National Budget and the Technical University of Civil Engineering Bucharest.*

PhD Thesis

Summary

Studies on the calculation methods of deep excavations

PhD Student
eng. Cătălin CĂPRARU

PhD Supervisor
Professor PhD Anton CHIRICĂ

BUCHAREST
2012

CONTENTS OF THE SUMMARY

1 Introduction

The increasing density of urban areas has made tall buildings with deep foundations a necessity. In these conditions the car parking and other facilities are located in their basements. The increase of the foundation depth of these buildings has generated the need for larger and stiffer retaining works. This trend is also reinforced by the need to found on stiffer soils and the one of creating underground areas for locating their utilities.

1.1 Scope and objectives of the research

The present research aims at analysing the influence of parameters that controls the performance of deep excavations from the point of view of the effects on the already existing neighbouring buildings. Bearing this in mind, the influence of the existing buildings upon the response of new excavations is analysed. Since the relation between the excavation and the neighbouring building is considered reciprocal, the effects of new excavations on the behaviour of neighbouring buildings are also taken into account. Furthermore, this research also analysis the influence of building type on its admissible deformation, induced by excavations in their vicinity, as well as the parameters variation for quantifying the performance of excavations with the building-excavation distance. Moving onwards, one can observe the relation between the overburden loads of the neighbouring building and the performance of excavations (expressed in terms of forces and lateral deformations of the retaining wall, as well as the prop forces).

The research is motivated by the problem regarding the performance of deep excavations in soft to medium soils such as the ones in Romania. Thus, there is a need to perform very good estimations regarding the soil displacements since this is a very important criterion for preventing the damage of neighbouring constructions and utility networks. Using nonlinear finite element analysis represents a rational technique which is frequently used in current practice as it can integrate constitutive models for simulating soils' real behaviour; it also takes into account the complexity of the various construction stages. The above-mentioned arguments motivate the choice made, that is – nonlinear finite element analysis which is also very useful in estimating the soil's response for deep excavations and the reciprocal relation between this and the existing neighbouring buildings.

2 The current stage of research regarding deep excavations calculation methods

This chapter presents a classification of the methods for calculation of excavation. Since the systemic analysis of excavation-neighbouring buildings conducted within the current research (and described in Chapter 6 of the thesis) was elaborated using FEM, this chapter also presents the theoretical framework regarding the use of this method in geotechnical engineering. Further on, the concepts regarding the design of retaining walls by conventional methods are presented. It is also described the provisions of national and European regulations regarding the deep excavation calculation and it ends with presenting the methods regarding the application of safety factors within the design of retaining walls.

3 The mechanical behaviour of soils

Chapter 3 presents the mechanic behaviour of soils under different stress paths. The stress-strain relationship of cohesive soils is different than the one for cohesionless soils, because in

both cases it is influenced by different factors (e.g. anisotropy stress path and mean principal stress). This is the reason why the behaviour under different load types is presented separately for clayey soils and sandy soils.

4 Constitutive soil models

Chapter 4 firstly presents a general definition of stresses and strains, in order to establish the basis for the constitutive soil models presented henceforth. Various constitutive soil models are presented in a systemized manner: some elasticity models (linear-elastic and non-linear elastic models) as well as some plasticity models (the well-known Mohr-Coulomb model and a model with two yield surfaces – i.e. the "Hardening soil model"). The aim of this description is the introduction of the constitutive models which are used in the FE analysis conducted for the parametric study in chapter 6 and for the case studies in chapter 7.

5 The influence zone of excavations

This chapter describes the influence zone of excavations, a very sensitive subject within the framework of current national norms. It describes the main factors which influence the displacements induced by excavations, the excavations' risk sources provided within the national in force regulations. Furthermore, a classification of methods used for estimating the influence zone of excavations (in special technical literature) is presented, as well as various criteria for estimating the damages of building subjected to excavation-induced ground movements.

Practical experience has occasionally dignified damage of the excavations' neighbouring building even though their stability was ensured. The economic losses made by damages of buildings are considerable and such incidents can usually expand the deadline for construction. Thus, the serviceability of the neighbouring structure is usually a key factor and plays a significant role in performance based design of excavations. In practice, any empirical, semi-empirical and numerical method can be adopted for evaluating the serviceability of the neighbouring building. The procedures used for estimating the possible damages of the neighbouring buildings through empirical and semi-empirical methods generally include three main elements:

a) Estimating excavation-induced ground movements;
b) Estimating excavation-induced deformations of neighbouring buildings;
c) Evaluating possible damage of neighbouring buildings based on excavation-induced deformations.

5.1 Possible factors affecting excavation-induced ground movements

The retaining wall and the supporting system of an excavation can be affected by a large number of factors, such as: the wall stiffness, its depth, ground conditions, groundwater table, the geometry of excavations, the different construction stages, the stiffness of the supporting system, workmanship etc. As reported in the previous studies (e.g. Hashash & Whittle, 1996; Kung et al, 2007b) the wall deflections and the ground movement are affected by many factors which may be grouped into three major categories (Kung, 2009), shortly presented henceforth.

5.1.1 Inherent factors

- Soil Stratigraphy: such as soil strength, soil stiffness, stress history of soil, and

groundwater conditions. In general, larger wall deflection could be induced for an excavation in soils with lower strength and stiffness.

- Site environment: such as adjacent buildings and traffic conditions. High-rise buildings and heavy traffic adjacent to the excavation site may lead to extra wall deflection.

5.1.2 Design-related factors

- Properties of retaining system: including wall stiffness, strut stiffness, and wall length. Larger wall deflection may be expected when using low-stiffness wall.
- Excavation geometry: including width and depth of excavation. Generally, the wall deflection is approximately proportioned to the excavation depth.
- Ground improvement: such as jet grouting method, deep mixing method, compaction grouting method, electro-osmosis method, and buttresses. The soil strength and stiffness could be strengthened by ground improvement, which may reduce wall deflection.

5.1.3 Construction-related factors

- Construction methods: such as the top-down method and bottom-up method.
- Over-excavation: Over-excavation prior to installation of strut may cause larger wall deflection.
- Duration of the construction sequence: the duration of the strut installation or the floor construction. For an excavation in clay, longer duration for installing the strut or constructing the floor slab may cause larger wall deflection due to the occurrence of consolidation or creep of clay.
- Workmanship: poorer workmanship may cause higher wall deflection.

5.2 Excavation-induced ground displacements

This section briefly presents the (semi-)empirical methods for estimating the soil settlement in the close vicinity of excavations and the features of ground displacements. Even though the literature in this field has advanced many empirical formulas just four of the most well-known methods will be presented.

5.2.1. Peck method

Based on field observation, Professor Ralph B. Peck (1969) was the first to advance a method for estimating the settlement induced by excavations. He mainly analysed the results of monitoring case studies in Chicago and Oslo and established a relation between the soil settlement profiles (δV) and the distance from the wall (d) for different types of soil, as it is presented in Figure 5.2.The method classifies the soils in three main categories:

- Type I: Sand and soft to hard clay;
- Type II: Very soft to soft clay:

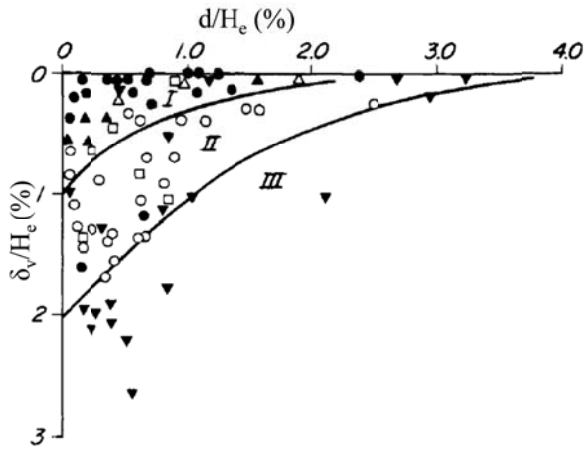

Figure 5.2 Peckk's Method for estimating excavation-induced soil displacements (after Terzaghi *et al.*, 1996)

a) Limited depth of clay below bottom of excavation;
b) Significant depth of clay below bottom of excavation, but with adequate factor of safety against base heave, dar Nb<Ncb

- Type III: Very Soft to Medium Cloy to a signifant depth below bottom of excavation and with low factor of safety against base heave, with $N_b \geq N_{cb}$;

where N_b represents the effective factor of safety against base heave ($\gamma H_e/s_u$) and N_{cb} is the critical factor of safety against base heave.

5.2.2 Bowles method

The method developed by Joseph E. Bowles (1968) described in this chapter is applicable to spandrel type settlement profiles**,** but this cannot be used for excavations whose settlement diagram behind the wall has a concave type.

5.2.3 Clough & O'Rourke Method

After analysing various case studies, Clough and O'Rourke (Clough & O'Rourke, 1990) have developed a few types of excavation-induced soil settlements envelopes. According to their studies, excavations in sandy soils and hard clays will tend to produce triangular settlement profiles, the maximum settlement being recorded next to the retaining wall. The maximum retaining wall lateral deflection and the soil settlement behind them have medium values in the range $0.2\%H_e \div 0.3\%H_e$, with a spread of data from the case studies analysed by the researchers, up to $0.5\%H_e$. The envelopes of excavation-induced soil displacements are presented in figures 5.4,a and 5.4,b, separated for different ranges of $2H_e$ and $3H_e$.

One emphasizes that the excavation-induced settlement profiles proposed by Clough and O'Rourke are only valid for displacements developed during excavation stages or strutting installation stages. Displacements caused by auxiliary construction processes (e.g. effects of wall installation or groundwater lowering inside the excavation pit or recharge of aquifers systems outside the excavation, etc.) were extracted from the available measurements for strictly representing deformations caused by excavation and propping installation.

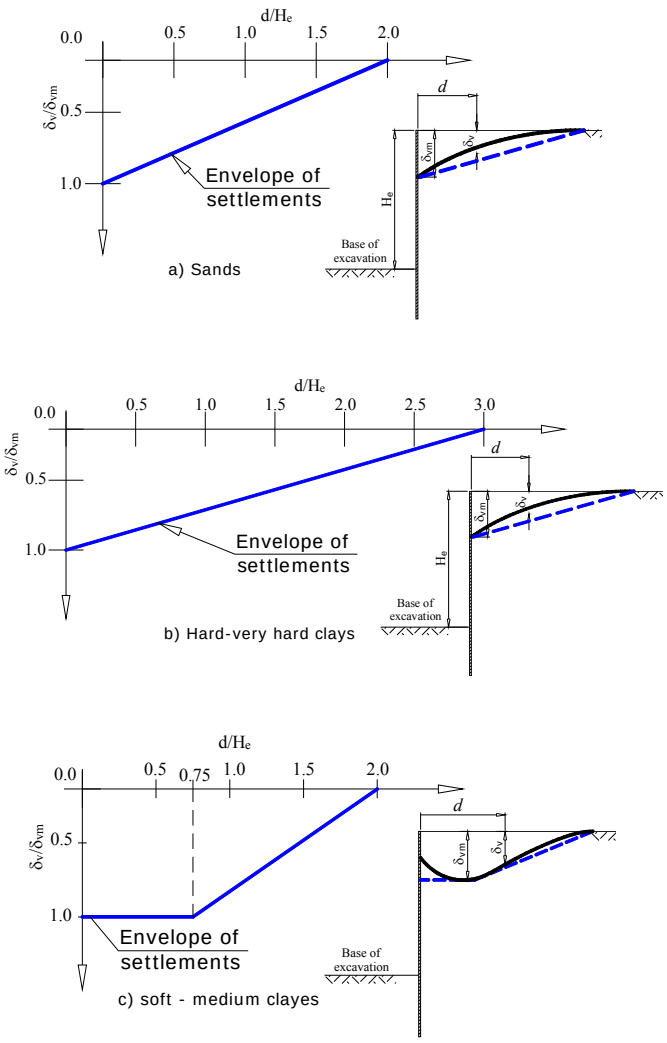

Figure 5.4 Design charts for estimating the distribution of surface settlement adjacent to excavation in different soil types (after Clough and O'Rourke, 1990)

5.2.4 Ou & Hsieh metod

Ou and Hsieh (Hsieh & Ou, 1998; Ou & Hsieh, 2000; Ou et. al., 2005; Ou & Hsieh, 2011) have developed a method for estimating excavation–induced soil profiles based on the study of soil settlement, influence zone, location of maximum settlement and the maximum magnitude of the settlements profile. They proposed the profile settlement presented in Figure 5.6.

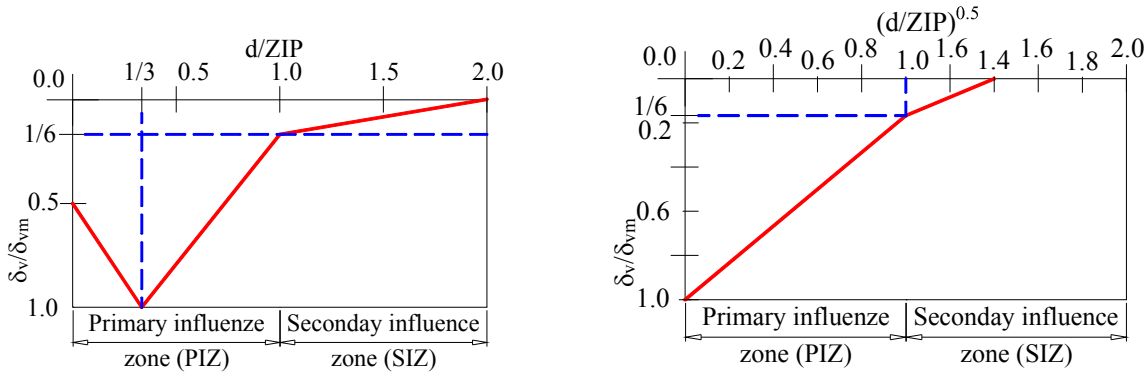

a) Concave type

b) Deformată de tip concav

Figure 5.6 Ou & Hsieh method for estimating excavation-induced soil settlements profiles (after Ou & Hsieh, 2011)

5.3 Damage approximation of buildings subjected to excavation induced displacements

5.3.1 Limiting deformation criteria

Boscardin and Cording (1989) concentrated on the tolerance of brick bearing walls and small frame structures to excavation-induced ground distortions and developed limiting deformation criteria to estimate their response. These types of structures were studied because they comprise a large portion of structures encountered around and near such excavations.

Boscardin and Cording (1989) quote a method initially developed by Burland & Wroth (1974), which models wall sections as elastic beams. Using this method, the effects of possible modes of deformation including bending, shearing, and combinations of both bending and shearing were studied on simplified wall sections. Limiting deformation criteria were developed by considering the effects of the bending and shear strains and including the effects of direct horizontal strains resulting from the corresponding excavation-induced ground movements.

The method developed by Boscardin and Cording (1989) is presented in Figure 5.12. This figure, which abscise is represented by the angular deformation β and the ordinate is represented by the tensile strain, ε_h, classifies the damage potential based on its intensity. The damage is established based on theoretical considerations regarding the structural answer to lateral strains, field observations of damaged buildings as well as measurements of vertical and horizontal differential displacements. A limited number of case studies were compiled in order to research the validity of the method as a basis for limiting deformation criteria. The levels of damage are based on the classification proposed by Burland et al. (1977).

Every curve that separates different levels of damage represents a certain value of critical tensile strain. Once the curves get closer to the minimum values of angular distortion, they become horizontal, representing the condition by which the specific horizontal deformation equals the critical one. When the curves approach the minimum values of lateral strain, this

represents an inclination by 45 degrees which represents the condition required for the diagonal tensile strain to reach the critical value.

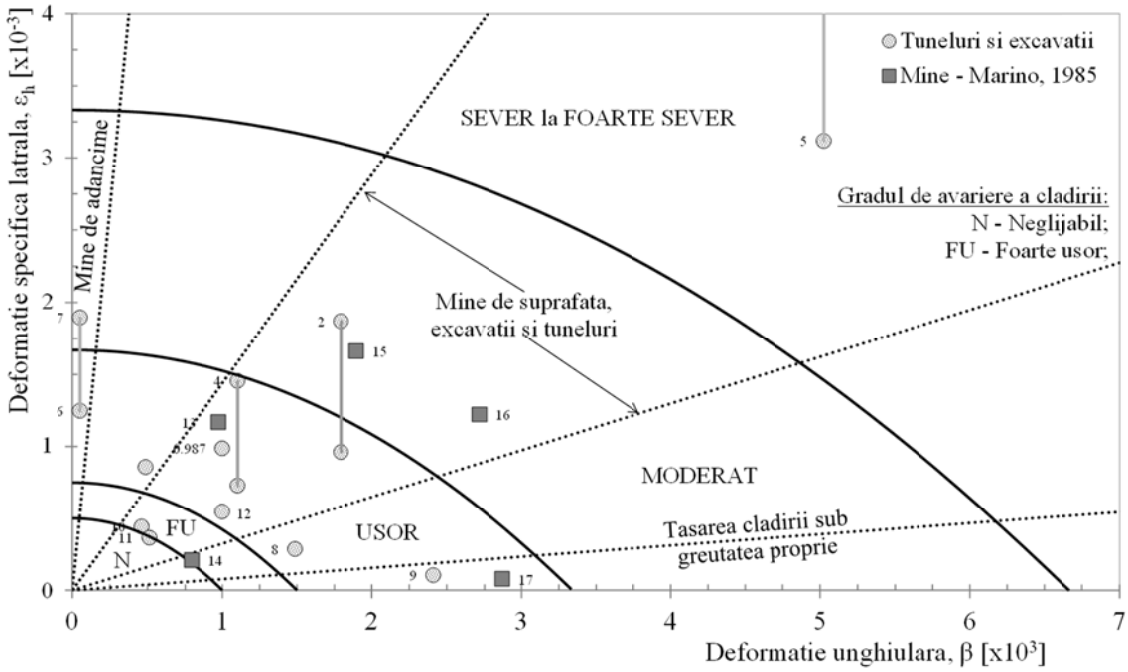

Figure 5.12:The relationship between the angular distortion and the critical tensile strain, for estimating the degree of damage(after Boscardin & Cording, 1989)

The limiting deformation criteria was developed taking into account the effects of pure bending and shear strains including the direct effects lateral strains which are generated by appropriate angular distortions induced by soil excavation.

5.3.2 Crack width approximation method

This method was proposed by Dulácska (1992) based on the diagonal strain in infill wall panels. For this he firstly developed the relation between relationship between ground and building distortions, by estimating the conditions on the infill wall panels.

During the excavation process, the ground surface settlement profile is constantly changing. As a consequence of this continuous process, the construction sections that initially occupied a deformation area could be placed, at the end of the process, in a different area. The identification of these areas is very important in estimating the damages due to the inherent differences of building sections applied forces, depending on the area where they are placed.

5.3.3 Strain superposition method

The damage approximation method was proposed by Boone (1996). To estimate the degree of damage of excavations' neighbouring buildings, this approach focuses on excavation – induced settlements profile's geometry induced, the geometry of structure and as the name of the method indicates it, on the strain superposition principle.

The procedure for determining the total crack width is developed using geometric formulas and the calculation of deformations of a uniformly loaded elastic beam. Based on these, using the end rotations of a wall panel, one can determine the bending and shearing strains. These components are then used in order to compute the principal strains. After that, the prin-

cipal strains computed for a certain wall panel are compared with the critical ones (proposed by Burland et al., 1977). If the calculated principal strains exceed the specified values, one passes to the next stage, otherwise it is assumed that no cracks will appear.

6 Systemic analysis of excavations

6.1 General issues

This chapter presents the analysis of the system composed of excavations and adjacent buildings by considering the soil-structure interaction. There will be analysed the parameters influencing the behaviour of excavations and their effects on the neighbouring built environment. These parameters involve the width of the excavation, the type bending stiffness of the retaining wall, the configuration and stiffness of the strutting system, the rigidity of the neighbouring buildings and last but not least, the distance between the excavation and the adjacent buildings. Thus, following the analysis, there will be discussed the influence of different factors affecting the behaviour of deep excavations in dense built areas.

The analysis was conducted by means of FEM, considering plane strain conditions. This method, unlike other calculation methods (such as limit equilibrium method or the beam on elastic foundation method) allows for estimating the forces and the displacements of the retaining structural elements and also for the diagnosis of stress and strain state induced in th soil.

For establishing the factors that influence the performance of deep excavations, we have created a geotechnical model of an excavation. This was done by statistical analysis of a database for retaining walls and ground movements due to deep excavations. Before being analysed, the database compiled in 2001 (Long 2001), comprising 296 case studies was extended by adding another 27 case studies. Some of these additional case studies were found in the special technical literature (after year 2001, for example Konstantakos, 2004 and Schweiger & Breymann, 2005), while others are represented in the case studies described in the next section of this paper.

6.2. Characteristic model's parameters

To understand the effects of existing buildings on new excavations' performance is necessary to determine a characteristic model to study the influence parameters. The parametric study aimed at identifying possible effects of neighbouring buildings on new excavations. The characteristic model parameters refer to: excavation depth, type of retaining wall, its depth and stiffness, strutting system configuration and stiffness, the height regime of neighbouring buildings (which also affects their rigidity) and the excavation-neighbouring building distance. All these features of the model, together with the soil layers an geotechnical parameters were determined based on the technical literature.

6.2.1 Excavation depth

Figure 6.4 presents the statistical distribution of case studies based on the excavation depth. To find the optimum distribution of case studies based on their excavation depth, the data was

grouped in consecutive series of 2m step. From the analysis of this figure, one can easily observe that for most of the case studies (approx. 83% - meaning 267 case studies) the excavation depth is comprised in the range 6÷20m. Moreover, the medium excavation depth is about 13m. Thus, the excavation depth of the characteristic model, was chosen to be H_e=13m

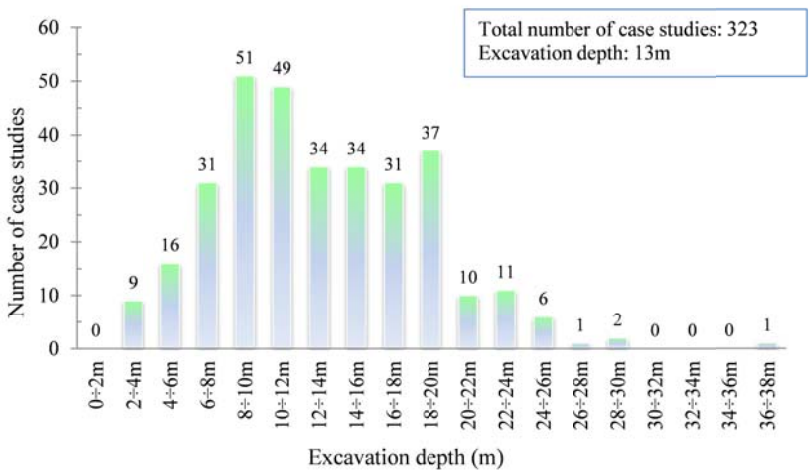

Figure 6.4 Distribution of the case studies based on their excavation depth

6.2.2 Retaining wall type and its bending stiffness

Figure 6.5 presents the statistical distribution of case studies based on retaining wall type. From this figure one can easily see that, among all the case studies in the extended database, the predominant type is the diaphragm wall (120 case studies meaning approximately 37%). This high percentage can be explained by the large stiffness of this type of wall compared to other retaining wall types.

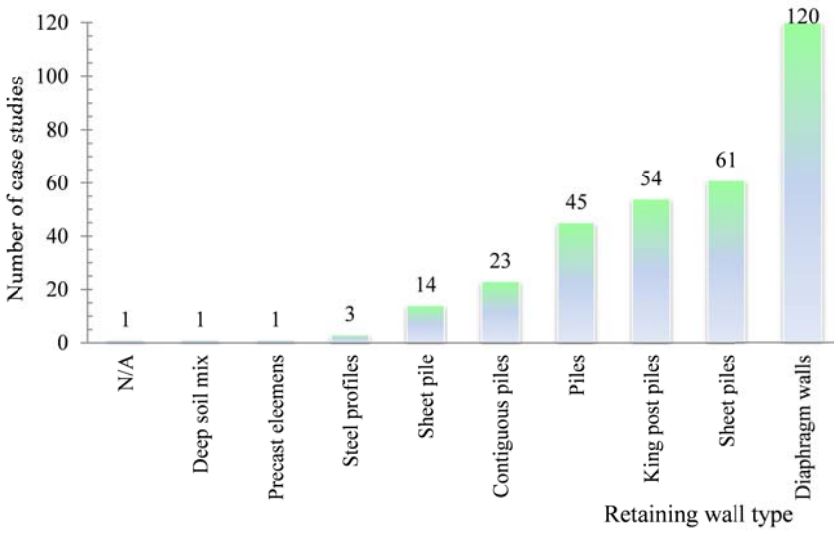

Figure 6.5 Distribution of the case studies based on their retaining wall types

Following extensive database analysis, the bending stiffness of the excavation retaining wall resulted in the value EI=1.75x106kNm^2/m

Based on investigations conducted by Woo & Moh (1990), the wall depth was set at H_p=1.8H_e ≈ 23.5m,

6.2.3 Configuration of the strutting system and distance between strutting levels

Figure 6.7 presents the statistical distribution of case studies based on the configuration of the strutting system. Among the types of excavations' support systems included in the extended database, most common are multiple levels of struts (about 50% - meaning 160 case studies), followed by multiple level of anchorages (about 20% - meaning 63 case studies). The high in use of multiple levels of props might be attributed to the ease of their installation and the fact that this type of support system allows for a greater ease in the technological sequence of op-

erations that occur in the excavation pits.

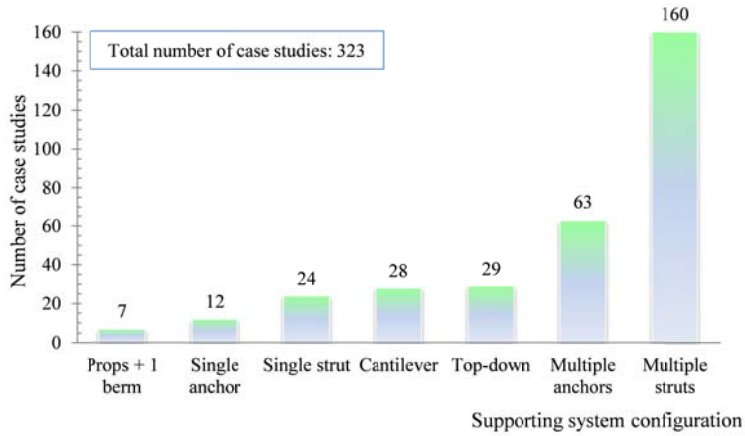

Figure 6.7 Distribution of case studies based on the supporting system configuration.

However, unlike some of the supporting types listed in Figure 6.7, the struts could add a substantial stiffness contribution to the supporting system of an excavation, even by placement at large in-plane distances (e.g. for 4÷8m).

From the facts presented above, for the characteristic geotechnical model it has been considered appropriate the choice of a supporting system consisting of multiple levels of struts, placed at a vertical distance of approximately h_s=4m. As the depth of excavation, previously established in Section 6.3.1 is 13m, there were considered 3 levels of struts placed at a vertical distance of 4m (i.e. EL-2m, EL-6m, EL-10m).

6.2.4 Neighbouring buildings

To analyse the characteristic model there were considered five types of buildings, with 1÷8 storeys, whose geometric characteristics are described in Table 6.2. For each story of the building a height of 3m and a dead load of 15kPa were considered appropriate.

Table6.2: neighbouring building parameters

Parameter		Type A	Type B	Type C	Type D	Type E
Material	(-)	Concrete	Concrete	Concrete	Concrete	Concrete
Unit weight, γ_b	(kN/m^3)	25	25	25	25	25
Number of storeys (n)	(-)	1	2	3	4	8
Storey height	(m)	3	3	3	3	3
Building height	(m)	3	6	9	12	24
Building length	(m)	20	20	20	20	20
Slab thickness	(cm)	15	15	15	15	15
Storey dead load	(kN/m^2)	15	15	15	15	15
Total building load	(kN/m/m)	37.5	56.3	75.0	93.8	168.8

The simulation of building behaviour was achieved by modelling it as a surface beam, taking into account both the bending stiffness and the axial stiffness of the building. In calculation of the bending stiffness as well as the axial stiffness of the surface beam, only the reinforced concrete slabs' rigidity was considered (ignoring the stiffness of vertical structural elements).

The model is proposed by Potts and Addenbrooke (1997). To study the influence of the stiffness of a building located at the ground surface on constructing bored tunnels, they used a surface beam model. The beam used to simulate the building was assumed to be elastic and its interface with the soil to be rough.

6.2.5 Soil stratigraphy and geotechnical parameters

For the characteristic model, the soil stratigraphy adopted in calculations is proper to the one for Bucharest. Data regarding this soil stratigraphy and geotechnical parameters were gathered from the technical literature (Saidel et al., 2010 and Tschughnigg & Schweiger, 2010).

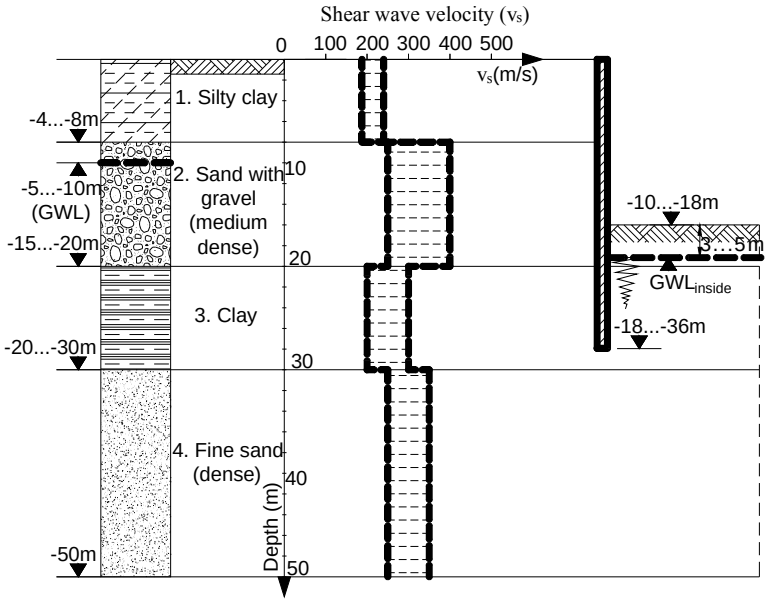

Figure 6.10 Geological profile for deep excavations in Bucharest (after Saidel et al., 2010).

For the general case of deep excavation, in which part of the soil encounters stress path changes due to loading and, constitutive soil models with two yield surfaces lead to proper results. In numerical analysis, this is achieved by part of the part of the mesh experiencing primary loading (in shear) and other part unloading. Such a constitutive soil model is the hardening soil model, presented in chapter 4.

Geotechnical parameters adopted in the calculations together with the thickness of layers are presented in Table 6.5. The groundwater level is located at a depth of 7m bellow the ground surface.

Table 6.5: Geotechnical parameters of the soil layers

Parameter		Meaning	Layer			
			Silty clay	Sand with gravel	Clay	Fine sand
h	[m]	Layer depth	6	12	7	25
γ	[kN/m^3]	Unsaturated unit weight	18	20	19	20
γ_{sat}	[kN/m^3]	Saturated unit weight	20	21	20	21
φ	[°]	Angle of internal friction	14	28	17	30
c	[kPa]	Cohesion	25	0	25	0
ψ	[°]	Dilatancy angle	0	0	0	0
ν_{ur}	[–]	Poisson ratio for unloading/reloading	0.20	0.20	0.20	0.20
E_{50}^{ref}	[kN/m^2]	Secant stiffness modulus in standard drained triaxial test	15000	30000	20000	35000
E_{oed}^{ref}	[kN/m^2]	Oedometric modulus	15000	30000	20000	35000
E_{ur}^{ref}	[kN/m^2]	Unloading/ reloading stiffness modulus	60000	90000	80000	105000
m	[–]	Power for stress dependency (acc. to von Soos, 2001)	0.7	0.6	0.7	0.5
p^{ref}	[kPa]	Reference pressure	100	100	100	100
$k_0^{(NC)}$	[–]	At rest earth pressure coefficient	0.700	0.530	0.750	0.500

6.2.6 Model boundaries

The model boundaries were settled based upon the recommendations issued by Bakker (2005). Geometry of the characteristic model is presented in figure 6.11.

6.2.7 Construction stages

Having established the all ingredients for the characteristic model, we need to define the construction stages taken into account for the FEM simulation. Thus, in this chapter, there are presented the construction stages.

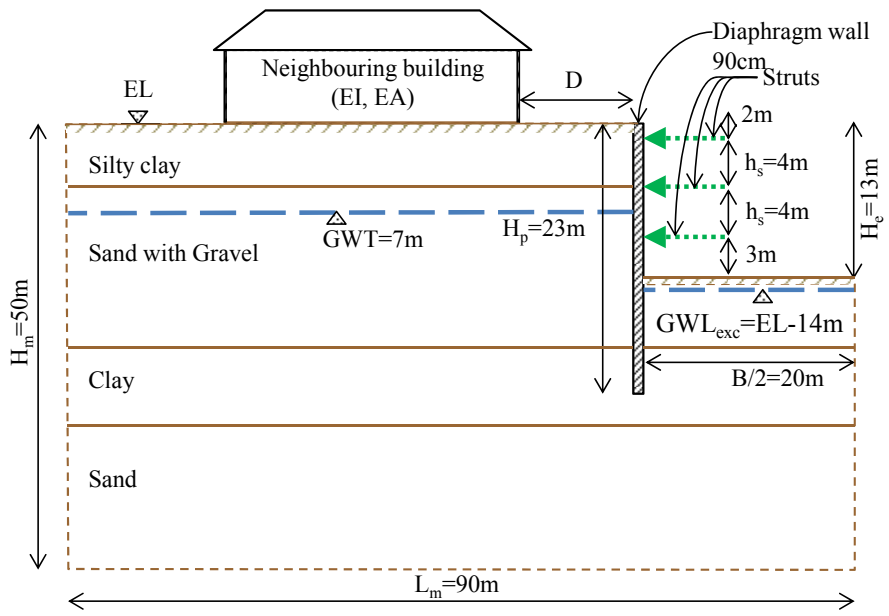

Figure 6.11 Characteristic model

6.3 Parametric study

The variables considered in the parametric studies were the overburden load of the neighbouring building, the stiffness of the building and the distance between the excavation and the neighbouring building.

Table 6.7 presents the distances between the excavations and the neighbouring building considered for the parametric study.

Table 6.7: Distances between the excavation and the neighbouring building considered in the parametric study

Case	D1	D2	D3	D4	D5	D6	D7
Distance (m)	1.3m (=0.1H_e)	2.6m (=0.2H_e)	3.9m (=0.3H_e)	5.2m (=0.4H_e)	1.3m (=0.5H_e)	10m (≈0.75H_e)	13m (=1.0H_e)

6.4. Results of the parametric study

This section provides the results of the parametric study by means of FEM analysis. To understand the effects of the existing buildings on designing new excavations and the influence of excavations on existing buildings, in the numerical analysis there were monitored following parameters: maximum lateral displacement of the retaining wall, settlements and angular deformations of the neighbouring building, lateral movements the building corners, ground surface settlement, maximum bending moment in the retaining wall, axial forces in the propping levels.

6.4.1 Displacements of the retaining wall

Figure 6.13 illustrates the lateral displacements of the retaining wall for building type A (1 storey) and for various distances excavation-neighbouring building. For the case when there is no building in the vicinity of the excavation, it can be seen from this figure that the maximum wall displacement is about δ_{hm}≈22m. A maximum lateral displacement of the retaining wall of δ_{hm}≈26m (an increase of about 18%) occurs in the case the building is positioned at a distance

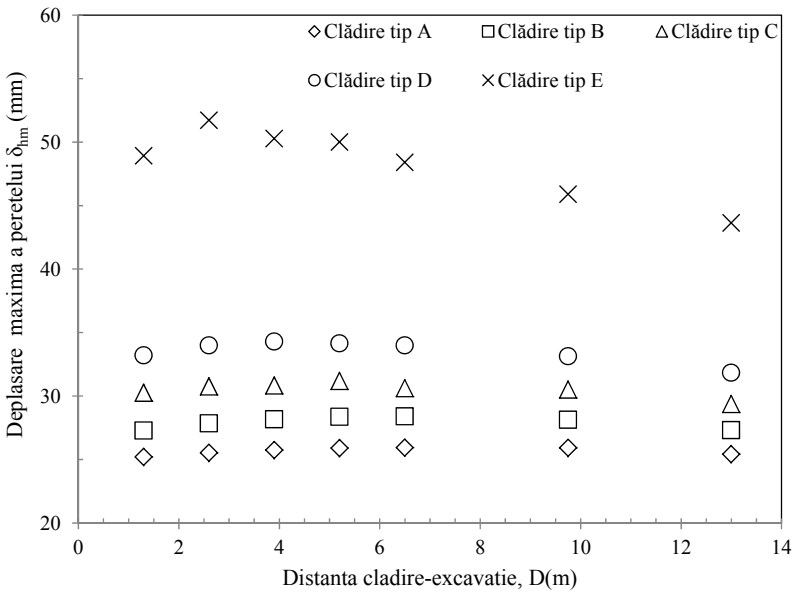

Figure 6.12 Variation of maximum lateral wall deflections with excavation-neighbouring building excavation.

D1(=0.1He=1.3m) from the edge of excavation. The variation of retaining wall's maximum horizontal displacements with excavation-neighbouring building distance, depending on the type of building (stiffness and overburden load) is represented in Figure 6.12. Following the normalisation of these values, with the excavation depth (graph represented in figure 6.14), one can observe that the relationship between the maximum lateral wall deflection (δ_{hm}) and the distance excavation- neighbouring building might be expressed by equation (6.4):

$$\left(\frac{\delta_{hm}}{H_e}\right) = a_i\left(\frac{D}{H_e}\right)^2 + b_i\left(\frac{D}{H_e}\right) + c_i \tag{6.4}$$

Where parameters a_i, b_i şi c_i depend, for a certain soil stratigraphy, on the type of neighbouring building and the overburden load.

Table 6.8: Values of coefficients a_i, b_i şi c_i for the characteristic model

Building type	a_i	b_i	c_i
A (1 storey)	-0.7152	0.1839	3.854
B (2 storeys)	-0.5371	0.444	2.5332
C (3 storey)	-0.3831	0.3361	2.3058
D (4 storeys)	-0.4262	0.4625	2.0616
E (8 storeys)	-0.2563	0.2992	1.912

6.4.2 Settlements of the neighbouring buildings

According data in the extended database, excavation induced settlement are known for 40% of the case studies (approx. 130 case studies representing. Thus, within the total available data, maximum settlements values are in the range 0÷600 mm, while for the case studies with diaphragm walls (120 case studies, as mentioned in Section 6.2.2) the maximum ground settlements are in the range 2÷220mm.

This clearly emphasizes a reduction of the settlement range which could be put on the diaphragm wall larger stiffness (compared to other retaining wall types reported in the extended database).

For the analysed characteristic model in this study, the values of maximum settlements of the neighbouring buildings have resulted within 6 to 48mm. By comparison with the values recorded in the extended database maximum building settlements are considered within the acceptable limits.

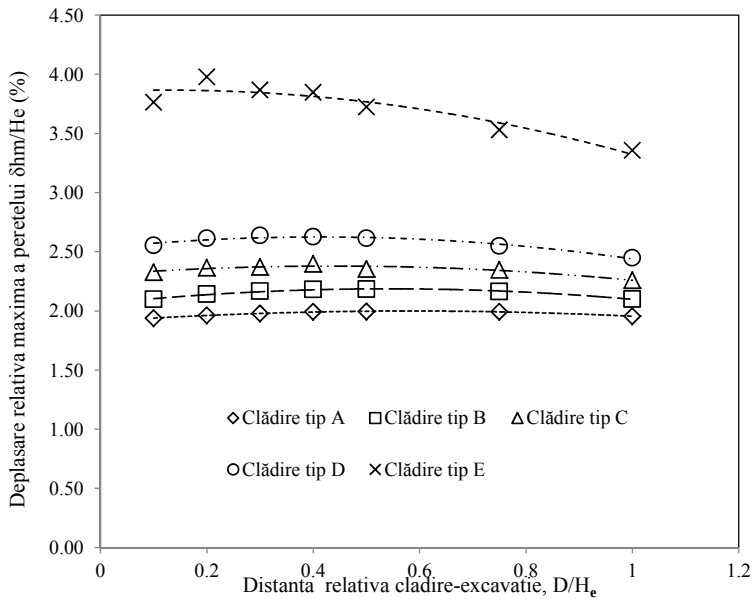

Figure 6.14 Variation of normalised maximum lateral wall deflections with relative distance excavation-building

From Figure 6.15 it is observed that, regardless of the building height, maximum normalized settlement (divided by the excavation depth) decreases with increasing distance excavation building. The gradient of this trend depends, in this case, on the rigidity of the building. The buildings whose flexural rigidity is higher (buildings with more than 1 storey, or for which the ratio length/height is smaller) encounter a greater settlement gradual decrease.

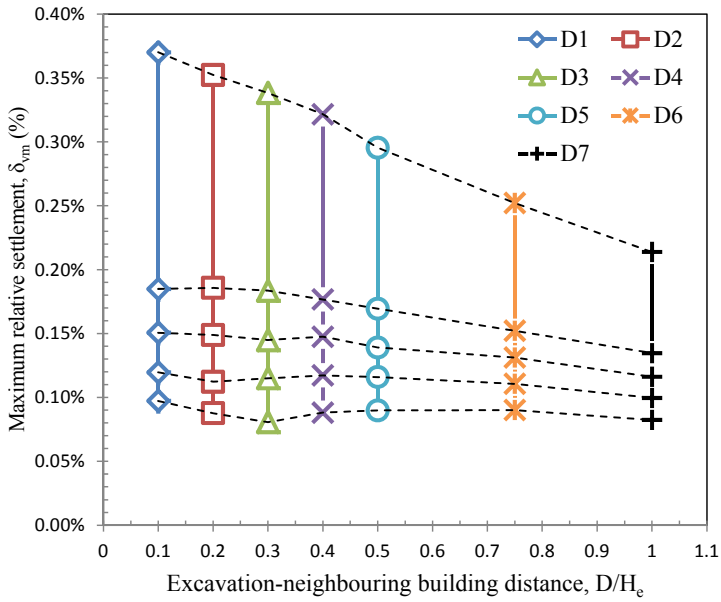

Figure 6.15 Variation of neighbouring buildings normalized maximum settlements with relative distance excavation-building.

Figure 6.16 presents the variation of maximum retaining wall deflections with maximum settlement is the maximum settlements. The purpose of this presentation is to validate the results achieved within the parametric study. As it can be seen in the figure, the values of maximum settlements resulting from numerical analysis, bordered within the range $0.4\delta_{hm}$ and $1.0\delta_{hm}$, while for the case study data recorded in the extended database, these limits are set between $0.4\delta_{hm} \div 3.0\delta_{hm}$, (there exists few cases for which these values are exceeded).

For a detailed analysis the reader is referred to Figure 6.17, where the values of normalized maximum settlements are plotted against the normalized maximum lateral displacements of the retaining wall. Figure 6.17 states that the case studies recorded in the extended database confined those for which the retaining wall consists in diaphragm walls.

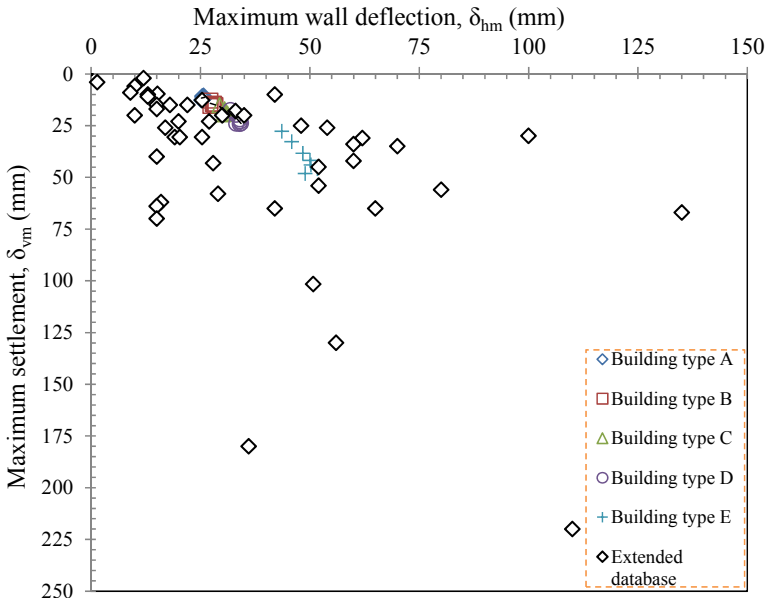

Figure 6.16 Variation of maximum retaining wall deflections with maximum settlement

6.4.3 The relation between the retaining wall lateral displacements and the neighbouring building settlements

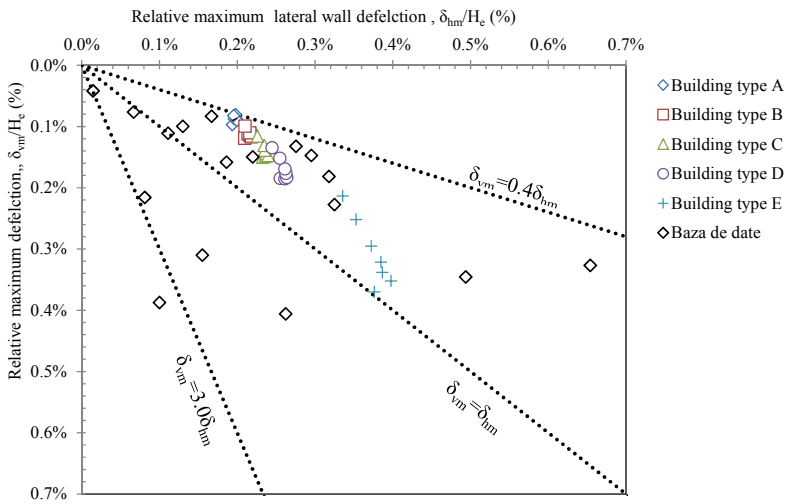

Figure 6.17 Normalized maximum retaining wall deflections with vs. normalized maximum settlement

Calculated lateral displacements were in the range 22mm (for the case with no neighbouring building) to 51mm (for building type E located at a distance D2 $=0.2H_e=2.6$m), while the maximum displacement recorded in the database were in the range 1÷160mm (for the 120 cases with diaphragm walls). All these aspects lead to the conclusion that there is a critical distance between the excavation and the neighbouring building $D_{cr}=0.1H_e \div 0.5H_e$ for which the buildings will record a maximum settlement and for which the retaining wall will record a maximum lateral deflection. This statement is also reinforced by the analysis of prop forces (described in the next section). Considering that the characteristic model resulted following a statistical analysis of a quite large database of excavations case studies, the results of the parametric are considered appropriate.

It should be noted, however, that each excavation is unique in its own way, through influencing factors (see Section 5.1 of Chapter 5). Therefore, it has to be conducted a detailed analysis of the influencing factors and the way they interact.

Analysis in terms of induced angular distortion β and tensile lateral strains ε_h of the neighbouring buildings leads us to the conclusion that: deep excavations, having a certain depth H_e, located at a distance smaller than $0.5H_e$ in relation to an existing building can generate a degree of damage included in classes *Negligible* to *Slight* (acc. to Table 5.2, after Burland & Wroth, 1975).

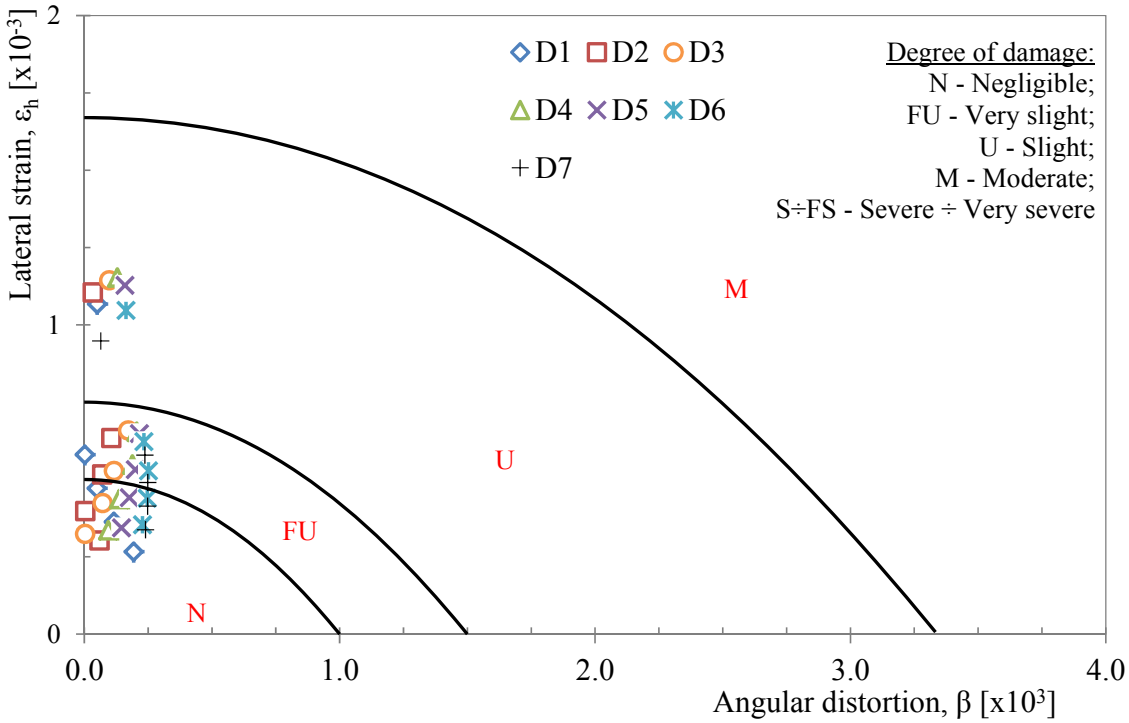

Figure 6.18 Evaluation of damage level for the neighboruing buildings considered in the parametric study (chart after Son & Cording, 2005)

To emphasize this, Figure 6.18 presents the positioning of excavation-induced degree of damage to neighbouring buildings. The chart is designed following the provisions of the limiting deformation criterion proposed by (Boscardin & Cording, 1989), and improved by Son and Cording (2005, 2010).

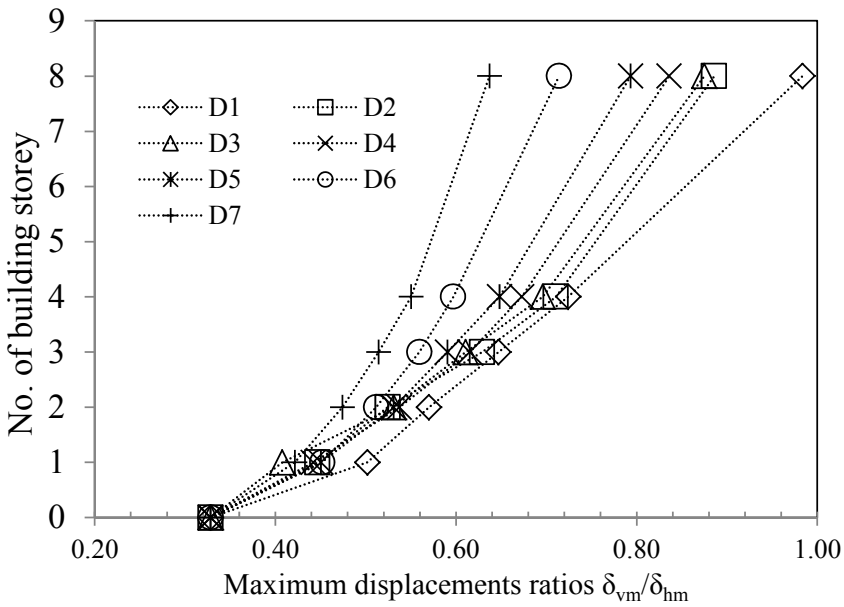

Figure 6.19 Ratio of the maximum settlement and the maximum lateral deflection of the retaining wall δ_{vm}/δ_{hm} versus the number of storeys of the neigh-bouring building

Conjoining the points in Figure 6.17, representing the calculated displacements for the characteristic model, will result in curves whose gradients define the maximum settlement

based on the retaining wall lateral deflection. We define this gradient as an *Excavation Influence Index* (c_{ie}). Figure 6.20 presents the variation of the excavation influence index with the number of storeys of the neighbouring building.

One may say that this index incorporates factors such as the building's weight (represented as an overburden dead load), its stiffness and excavation-neighbouring building excavation distance. To formulate the basis of this index, Figure 6.19 plots the ratio of the maximum settlement and the maximum lateral deflection of the retaining wall versus the number of storeys of the neighbouring building. It should be mentioned that zero levels (in Figure 6.19 and 6.20) represent the case where there is no building in the vicinity of a new excavation.

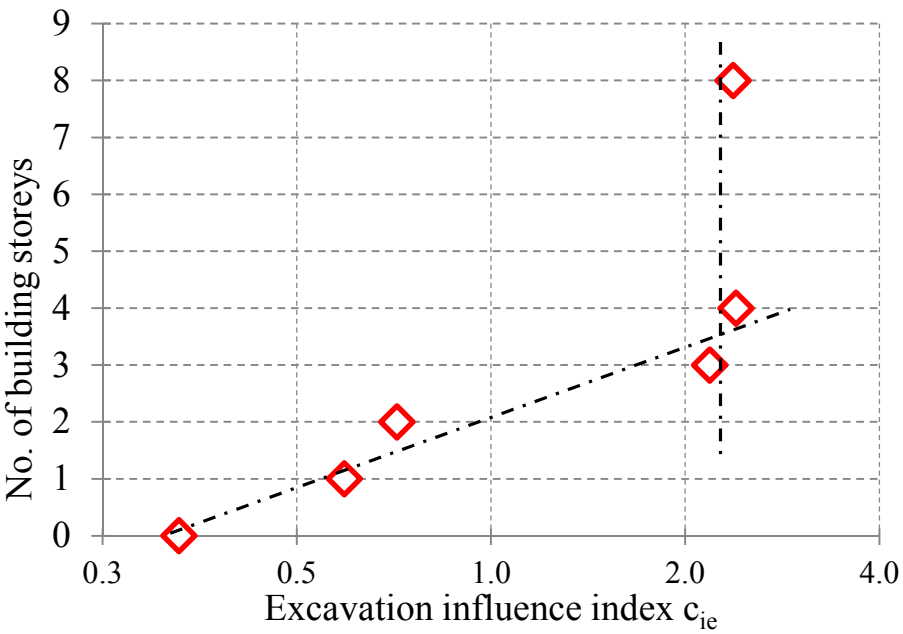

Figure 6.20 excavation influence index vs number of storeys of neighbouring buildings

6.4.4 Forces in the structural elements of the supporting system

This section presents the results of the parametric study regarding the forces of retaining wall (bending moments) and strutting levels (axial forces). We will analyse their variation with the excavation-neighbouring building distance. Figure 6.21 presents the bending moment diagrams for the retaining wall in the case of the neighbouring building is represented by a building type A (1 level).

The minimum bending moment M_{min}=671kNm/m corresponds to the case there is no building behind the retaining wall.

The maximum bending moment in the retaining wall is recorded in the case of building type E (8 storeys) located at distance D_5(=0.5H_e=6.5m) behind the excavation pit, as reported in figure 6.22.

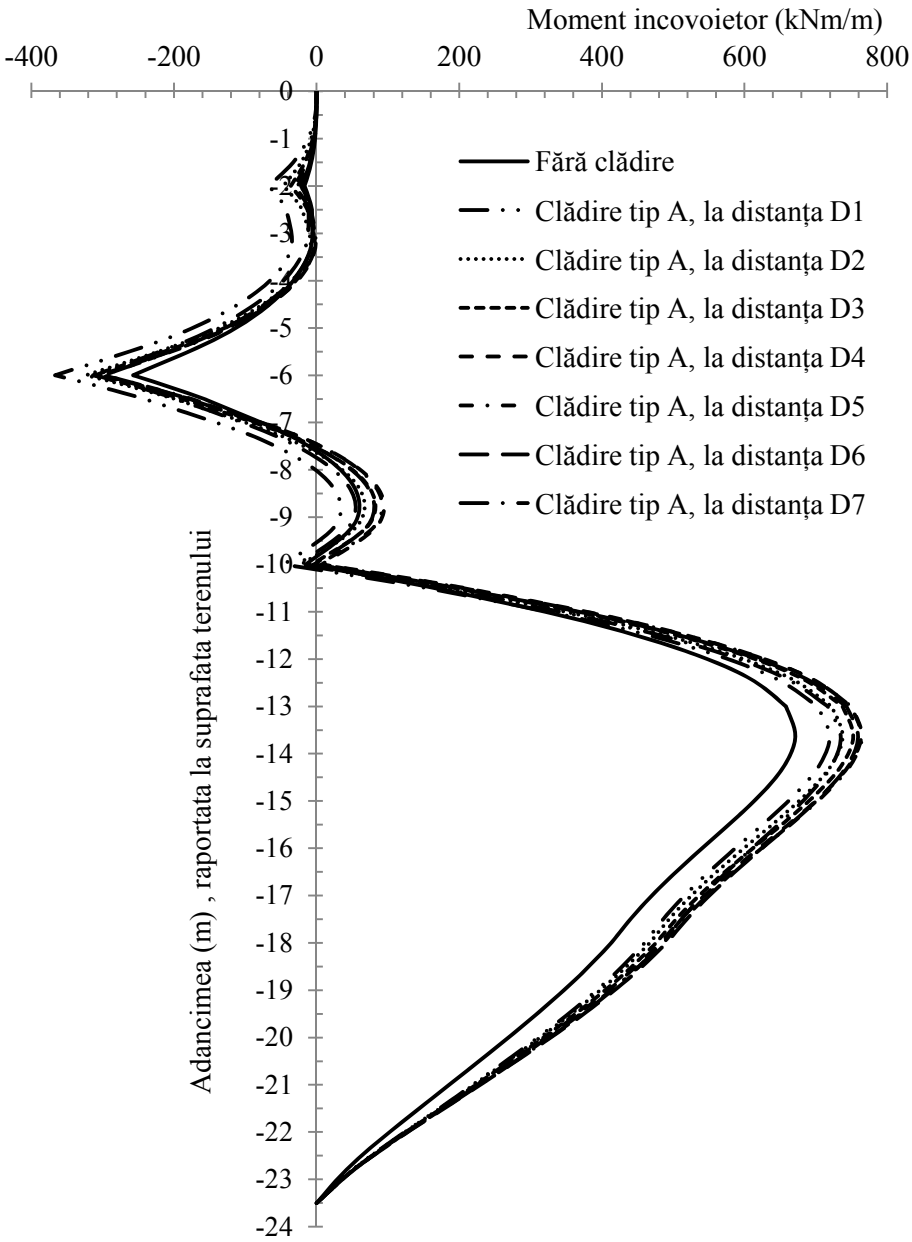

Figure 6.21 Lateral retaining wall deflections vs. depth, for a neighbouring building type A

Figure 6.23 reveals the variation of the axial force in the first props (EL-2) with the distance between the excavation and the neighbouring building. As it was expected to be, it can easily be observed from this figure that the maximum force is obtained for a building type E located at distance D1(=0.1H_e=1.3m) behind the retaining wall, while the minimum force is obtained for the case where there is no building behind the retaining wall.

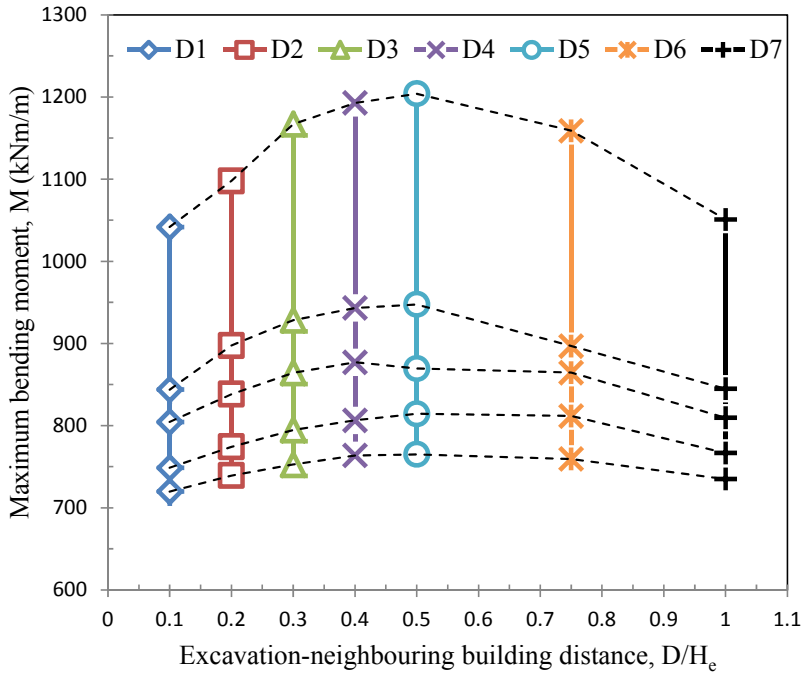

Figure 6.22 Maximum bending moment in the retaining wall vs. excavation-neighbouring building distance

At the same time, Figure 6.23 reveals a slight gradient (the hatched line) of the axial force, reducing at the same time with increasing distance excavation-neighbouring building.

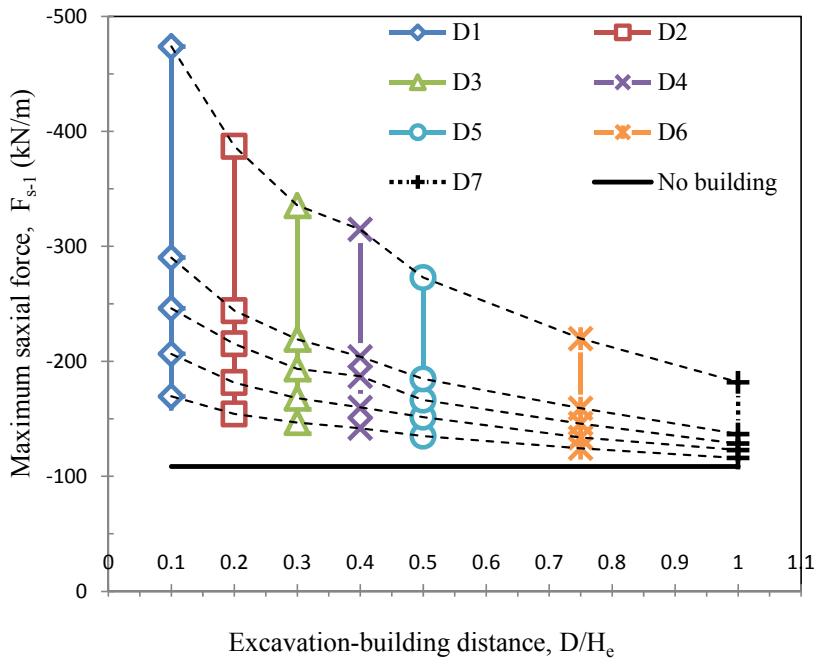

Figure 6.23 Maximum axial force in the first strutting level vs.excavation-neighbouring building distance

7 Case studies

This chapter presents the analysis conducted through FEM of three deep excavations (2 of them in Bucharest, Romania and one in Vienna, Austria). At the same time one emphasizes the advantages of using non-linear numerical analysis for estimating the soil behaviour in case of excavations. This is important for estimating a proper soil response in case of such geotechnical works, and for predicting their performance. According to the results of the parametric study described in the last chapter, this may offer the necessary tools for controlling the effects of excavations on the already built environment (quantified through the magnitude of the induced soil movements – translated into building distortions).

7.1 Case study EOD (Vienna)

7.1.1 Project Description

This case study is represented by a deep excavation endorsing the car parking of the EOD Towe in Vienna, Austria. The site of the excavation is located close to the centre of Vienna. The excavation depth is almost 21m (from about 7.8mWN down to about -13.2mWN), its area being of about 2400m^2.

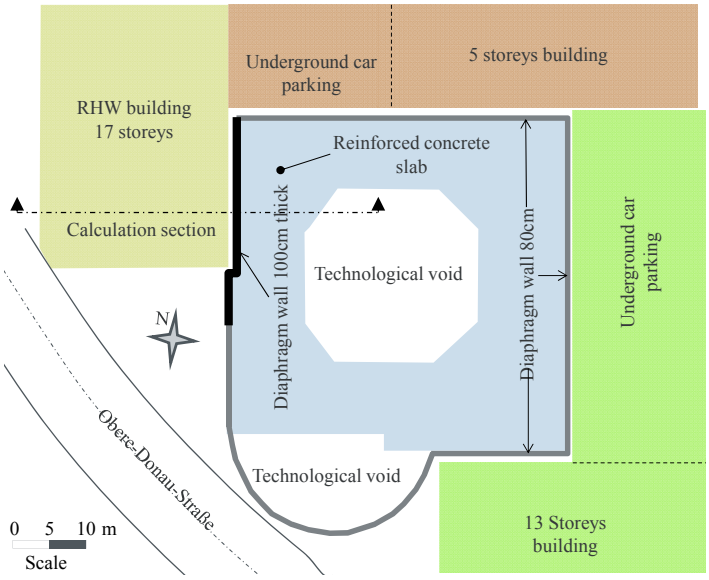

Figure 7.2 Location of the EOD excavation site

Due to the complex conditions encountered on site (i.e. high-rise neighbouring buildings) the designer has adopted the top-down procedure for the execution of the excavation, this being considered as the most adequate construction method for the project. The retaining structure consisted in a diaphragm wall with a thickness of 0.8÷1.0m which was supported, during the excavation, by the basement slabs (30÷40cm reinforced concrete slabs) executed through the "top-down" procedure.

The location of the excavation site is presented in Figure 7.2. The purpose of the present work was to analyse the section adjacent to RHW building (Figure 7.2).

7.1.2 Soil stratigraphy and geotechnical parameters

According to the geotechnical investigations on site and technical literature (e.g. Dölerl *et al.*, 1976), the soil stratigraphy consists of three main layers: quaternary gravel (~13m thickness), tertiary sand (~13m thickness) and tertiary sandy silt (down to about 60m).

7.1.3 Calculation hypothesis

This section briefly presents the hypotheses which were adopted in the calculation of the retaining wall and for evaluating the stress-strain state in the soil. The calculation is based on numerical methods and it was conducted by the following two methods:

- Beam on elastic foundation method: the calculation was conducted using the software "DC Pit" ("DC Baugrube"). The soil behaviour is modelled by elastic springs having a

certain constant limit value. At the end, there has been done a short comparison of the results by applying various approaches and safety factors provided in different European Norms, such as the Austrian Norm (ÖNorm 1997-1), German Norm (DIN 1054:2005), British Norm (BS 8002:1994) and the Swiss Norm (SIA).

- Finite element method: the calculation was conducted by using the software PLAXIS 2D and PLAXIS 3D. The analysis was conducted in both drained and undrained conditions using the Mohr-Coulomb model and the Hardening soil model for simulating the mechanical behaviour of the soil.

7.1.4 The geotechnical model

Figure 7.9 depicts the geometry of the model.

7.1.5 Results of the numerical analysis

7.1.5.1 Beam on elastic foundation method

To calculate excavation retaining wall (structural forces estimation) there has been used DC Pit software, modelling the soil by springs (characterized by a certain spring constant, k_s). Figure 7.10 depicts the geometry of the model.

Figure 7.11 presents the variation of the subgrade reaction modulus and in Figure 7.12 are presented the retaining wall lateral deformation diagrams, calculated according to several international standards. From this figure it is noted that the maximum wall deflection ranges from 26mm (according to calculations made by the provisions of ÖNORM EN 1997-1) and 53mm (according to SIA 267:2003). Noteworthy is the similarity between the results obtained by application of DIN 1054:2005 (identical to ÖNORM EN 1997-1) and BS 8002:1994. The behaviour of the retaining wall (from the point of view of its displacements) is very similar, the difference between the maximum horizontal displacements being of approximately 12%

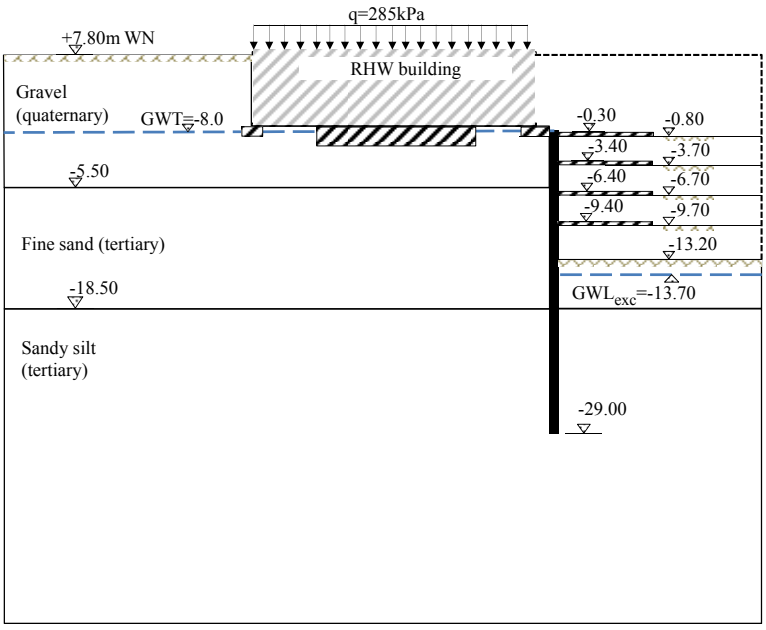

Figure 7.9 Geometry of the calculation section

The above mentioned aspects are also found in the retaining wall embedment depth. This was calculated based on the static equilibrium of forces acting on the wall (active and passive pressure and forces in the 3 strutting levels), and applying the safety factors provided by different norms resulted in: 23.76m (acc. ÖNORM EN 1997-1) 24.64m (acc. BS 8002:1994) and 23.26m (acc. SIA 267:2003). It should be noted that the differences between the retaining wall's embedment depths calculated acc. to the provisions of the three different standards are negligible (less than 6%).

7.1.5.2 Finite element method

In the previous section we have presented the results of numerical analysis using a pro-

gram that is based on beam on elastic foundation method. Major shortcoming of this method is that it cannot provide estimations regarding the excavation-induced ground movements. This is particularly important for the project in question, estimating the deformations induced to the neighbouring building RHW.

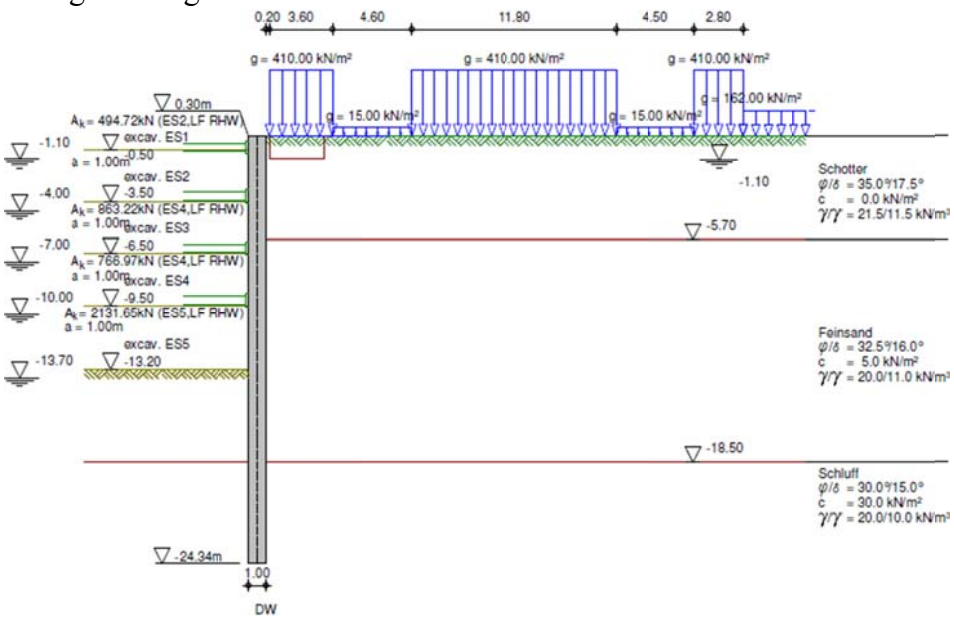

Figure 7.10 Geometry of beam on elastic foundation method's model

In this regard, advanced numerical calculations allowed us to estimate the stress and strain state induced in soil by the excavation. For this we used PLAXIS 2D program, whose results are presented in the following paragraphs. Geometry of 2D calculation model is shown in Figure 7.15. Figure 7.16 presents the excavation induced horizontal displacements diagram in the soil mass. From this it can be seen that the maximum horizontal displacement has a value of 40.8mm, recorded at a depth 16.2mWN (with 3m below the excavation).

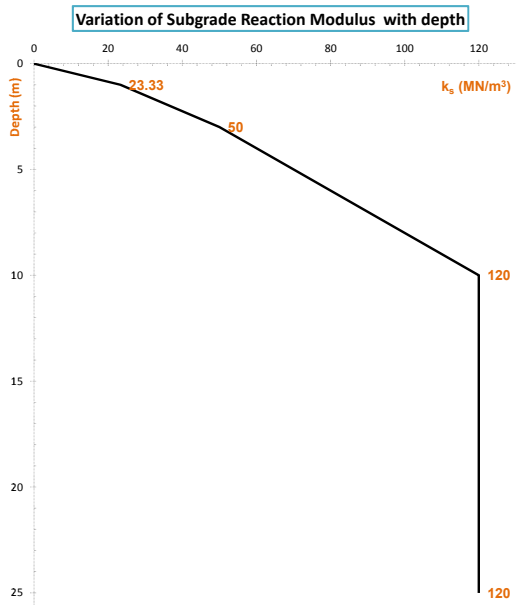

Figure 7.11. Subgrade reaction modulus

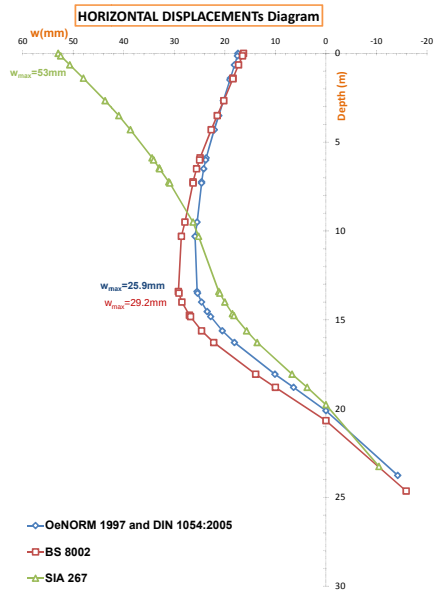

Figure 7.12. Lateral deflection of retaining wall acc. to the provisions of different standards

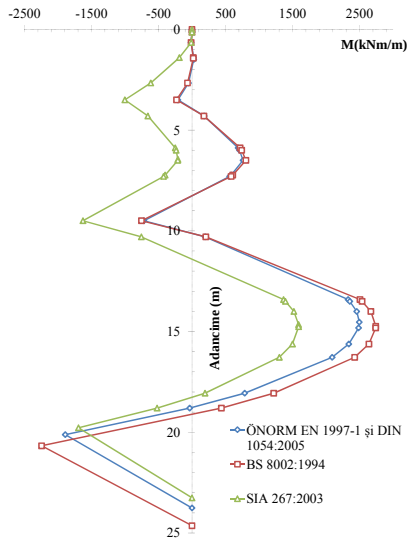

Figure 7.13. Design bending moments of retaining wall acc. to the provisions of different standards

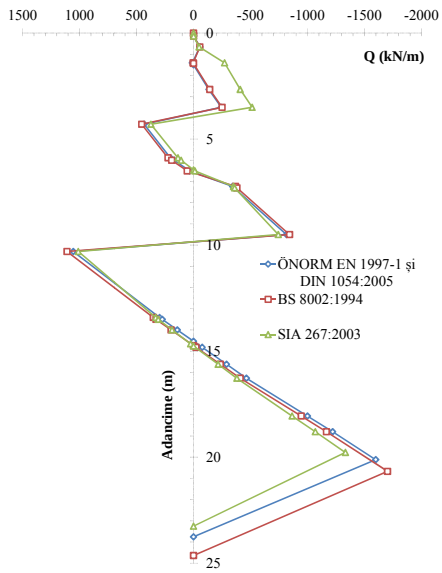

Figure 7.14. Design shear forces of retaining wall acc. to the provisions of different standards.

The ratio between the maximum settlement behind the retaining wall and the maximum lateral displacement of the wall equals δ_{vm}/δ_{hm}=0.4. This value follows the trend described in section 6.4.3, i.e. the ratio is bordered in the range 0.4 ÷ 1.0δhm.

Figure 7.18 presents the horizontal displacements of the retaining wall for each construction stage considered in the numerical simulation of the excavation

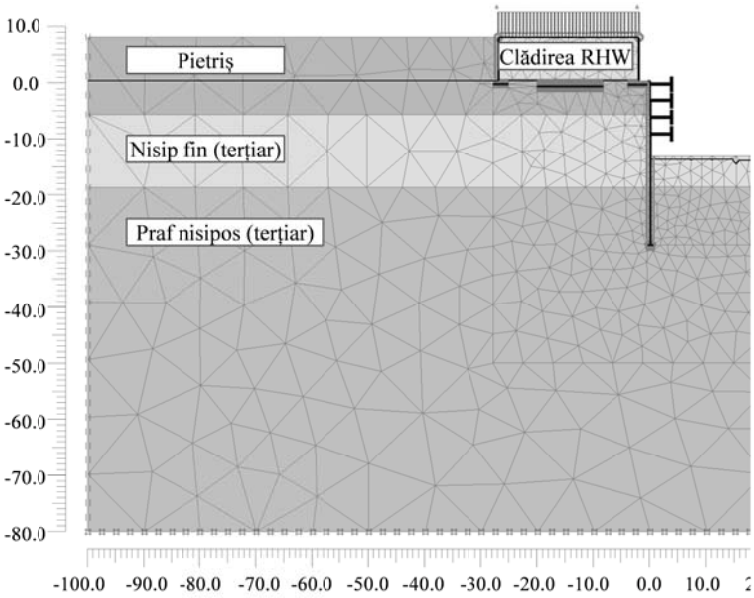

Figure 7.15 Geometry of the 2D FEM

It should be noted that of particular importance for estimating the state of stress and strains are the initial conditions on site (initial stresses in soil) prior to excavation. Since the soil layers are overconsolidated, several methods were used for simulating the initial conditions: at rest earth pressure coefficient and by using the overconsolidation pressure specified in the geotechnical report (σ'_p=560kPa). Proper results were obtained using the second method, i.e using the overconsolidation pressure, as specified in the following sections.

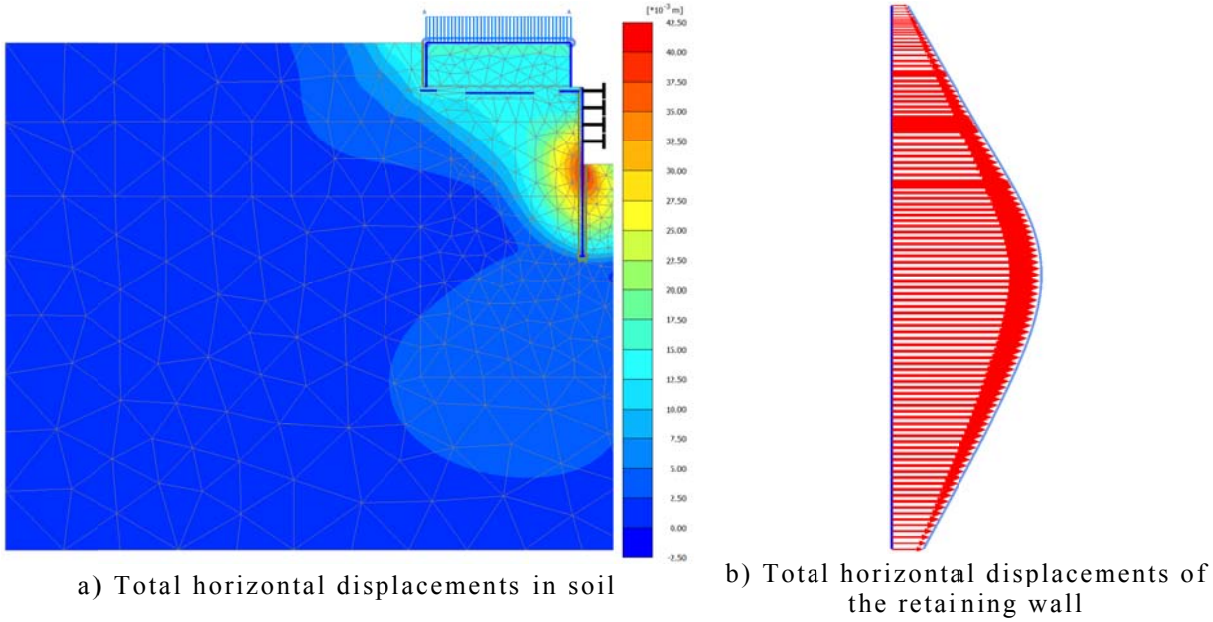

a) Total horizontal displacements in soil

b) Total horizontal displacements of the retaining wall

Figure 7.16 Excavation induced horizontal displacements

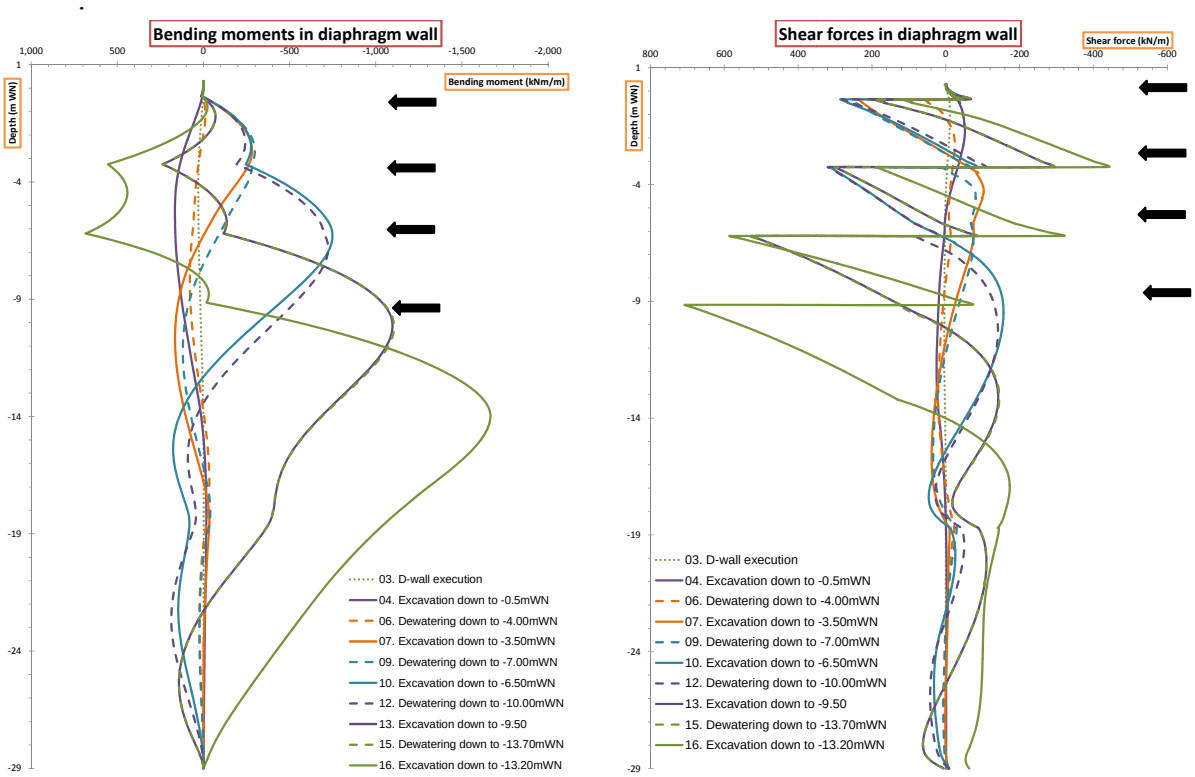

Figure 7.18 Structural forces in the retaining wall (for all construction stages in the numerical simulation of the excavation)

7.1.5.3 Analysis of supporting slabs

There were made variations regarding the stiffness of the slab-struts. The bending deflections of the slabs was analysed by means of finite element modelling, using the software Axis VM Lite. The stiffness of the slabs was iteratively computed by means of formula (7.5), the tolerated error being 10%.

$$EA_{placa,i+1} = \frac{F_i \cdot L_{placa}}{\delta_i} \tag{7.5}$$

where: $EA_{placa,\ i+1}$ – stiffness of the slab for iteration "i+1"; L_{placa} – length of the slab; F_i - Force in the slab in iteration "i", resulted from PLAXIS; δ_i - The medium bending deflection of the slab, resulted following the calculation with Axis VM, in iteration "i".

7.1.5.5 The initial pre-consolidation stress

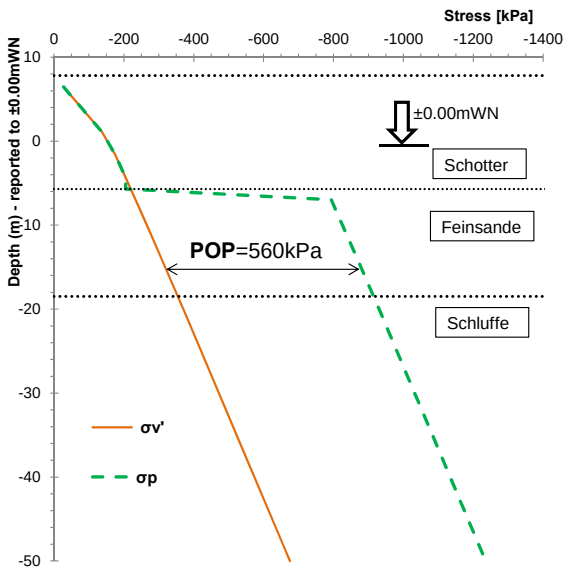

Figure 7.20 Illustration of vertical pre-consolidation stress in relation to the in-situ vertical stress

The vertical pre-consolidation stress σ_p is used to compute the equivalent isotropic pre-consolidation stress, p_{eq}, which determines the initial position of a cap-type yield surface in the advanced soil models, such as the hardening soil model described in section 4.5.2.

Using pre-consolidation stresses resulted proper horizontal and vertical deformations. As it can be observed in Figure 7.21, the measured maximum horizontal displacement of supporting wall is 9mm and the settlement behind it is 9mm. Using pre-consolidation stresses, the maximum calculated lateral displacement is 33.1mm (compared to 40.8mm calculated using K_0 – procedure) while the maximum settlement behind the wall is 12mm (compared to 16.8mm calculated using K_0 – procedure).

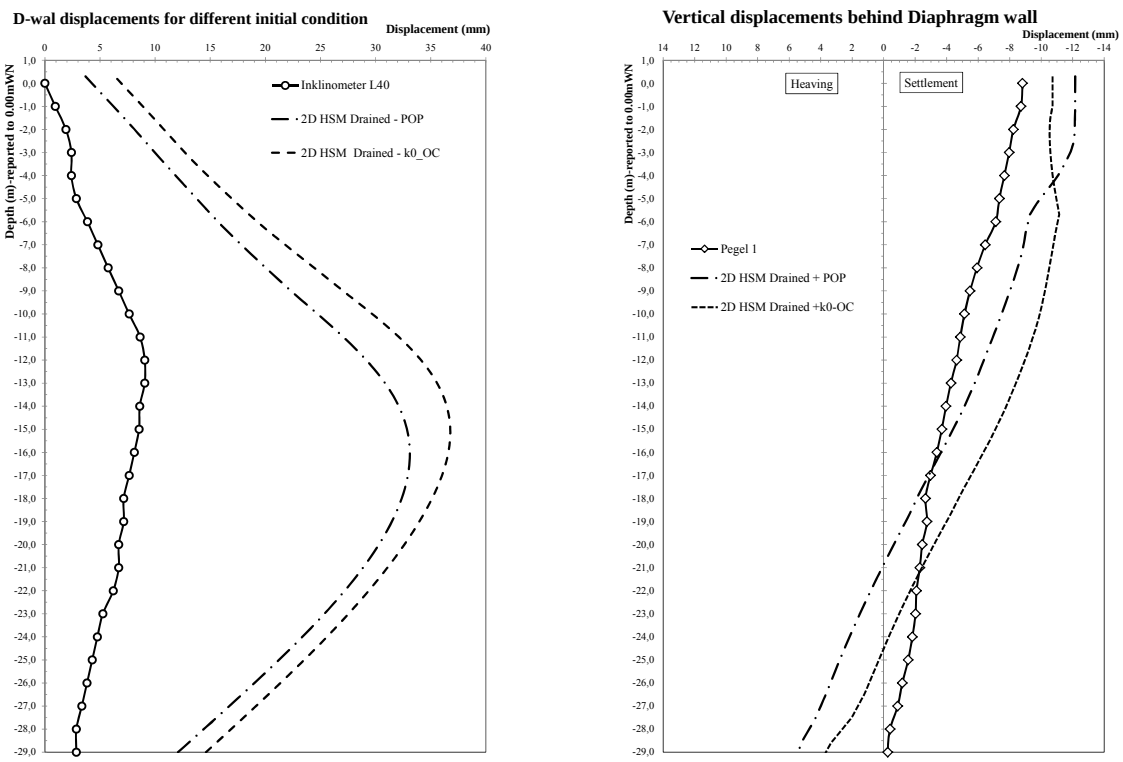

Figure 7.21 Comparison of displacements for different inputs of initial condition input (all in 2D analysis)

7.1.5.6 Influence of corner effects

Ou, et al. (1996) defined a Plane Strain Ratio ($PSR=(\delta_{hmax})_{3D}/(\delta_{hmax})_{2D}$) for a evaluated section of diaphragm wall, to quantify the restraint potential of wall corner. In which, $(\delta_{hmax})_{3D}$ and $(\delta_{hmax})_{2D}$ denote the maximum lateral wall movements from 3-D and 2-D analyses at certain excavation stage. The cross section being evaluated with higher PSR value represents the section is less restrained by wall corner and it may approach to plane strain condition as the PSR value becomes unity.

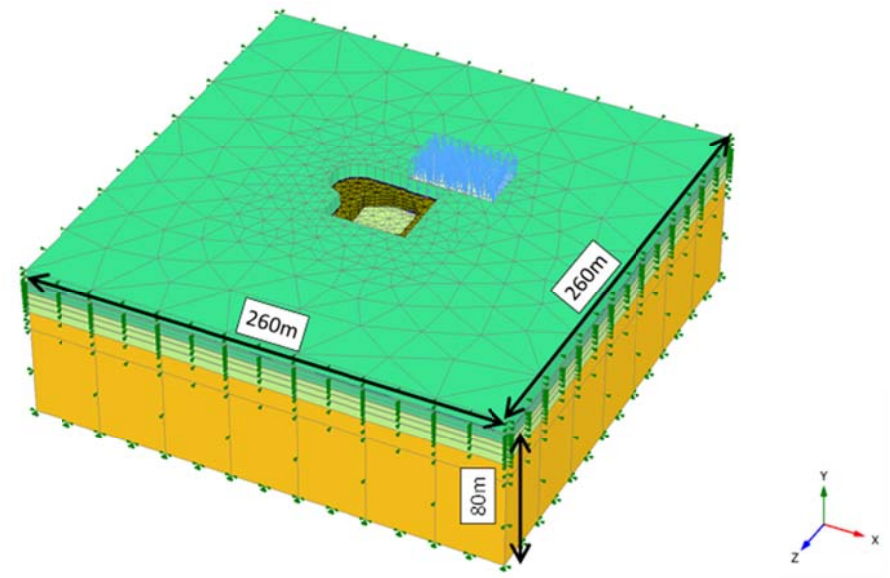

Figure 7.22 Geometry of the 3D EOD FE model

For determining the PSR for the current case studies there has been conducted a 3D drained analysis using the PLAXIS Software. The soil profile and geotechnical parameters used for the 3D Modelling are the ones provided in previous sections, though, for the initial conditions there has been used the POP procedure as shown in section 7.20. “The initial pre-consolidation stress”. The 3D model is presented in figure 7.22.

The results of the 3D numerical analysis are compared to the ones of the 2D calculation and the PSR is established, estimating the influence of corner effects. The results are illustrated in Fig..

As it can be observed from figure 7.23the plane strain ratio for the current case PSR=0.875 which concludes to the fact that the restraint potential of wall corner is quite diminished and that the 2D plane strain analysis conducted for the current section (Cross section C – located near the RHW building) leads to proper results.

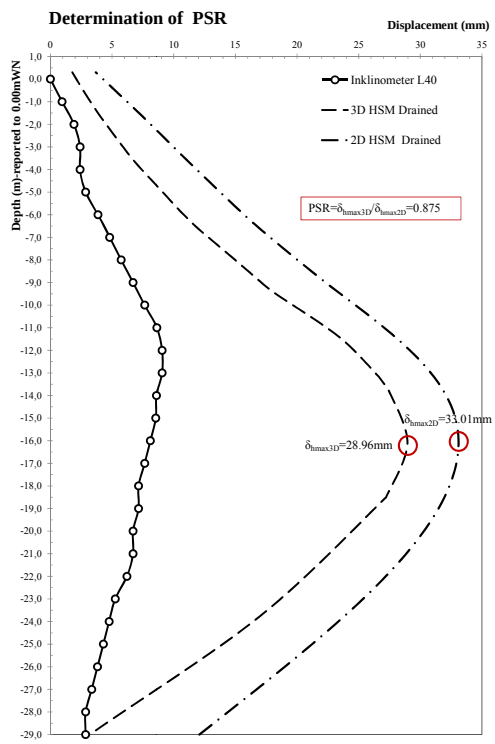

Figure 7.23 PSR determination for the EOD excavation

While the PSR value (0.875) indicates a low restraint potential of the corner effect, the differences between the horizontal displacements of the diaphragm wall computed in 2D and 3D vary in the range 15%÷37%. Though, the vertical displacements of the soil behind the retaining wall computed in 3D are a bit erroneous showing only a heave of the soil. This has also an implication on the

predicted behaviour of the neighbouring building, for which the measurements conducted on site indicated a settlement of about 9mm while the 3D modelling indicates a heave of about 5-6mm. This can be put on the use of the Mohr-Coulomb model for simulating the infrastructure of the RHW building (as it is known from the special literature, the MC model tends to predict erroneous heaving behaviour for the soil behind excavations – Schweiger, 2008) and the simplified simulation of other loading conditions on site.

7.1.5.7 Undrained analysis

An important aspect of the numerical analysis of an excavation is the drained or undrained behaviour. Generally, the drained analysis places the results on the safe side. Due to the fact that the stress path is unloading, the mean effective stress decreases, implying that the soil strength depends on the consolidation phenomenon, being a time function. In case of small excavations the site works are completed relatively fast and there will notice that the earth will resist without the need of any support system. But if there are delays in execution of works, unsupported vertical walls of these excavations will collapse, due to consolidation and water evaporation effects. Unlike embankments, for which the main stress path is primary loading and an undrained analysis is a safe approach, a drained analysis represents the safe approach for excavations. To highlight these issues, the analysis was performed both for drained and undrained conditions (adding a consolidation stage at the end of the analysis).

According to Wehnert (2006), when performing undrained analyses with numerical methods, a choice generally has to be made how the analysis is performed. The options consist in:

- Analysis in terms of effective stresses and effective strength and stiffness parameters (Method A);
- Analysis in terms of effective stresses using undrained strength parameters but effective stiffness parameters (Method B);
- Analysis in terms of total stresses using undrained strength and stiffness parameters (Method C).

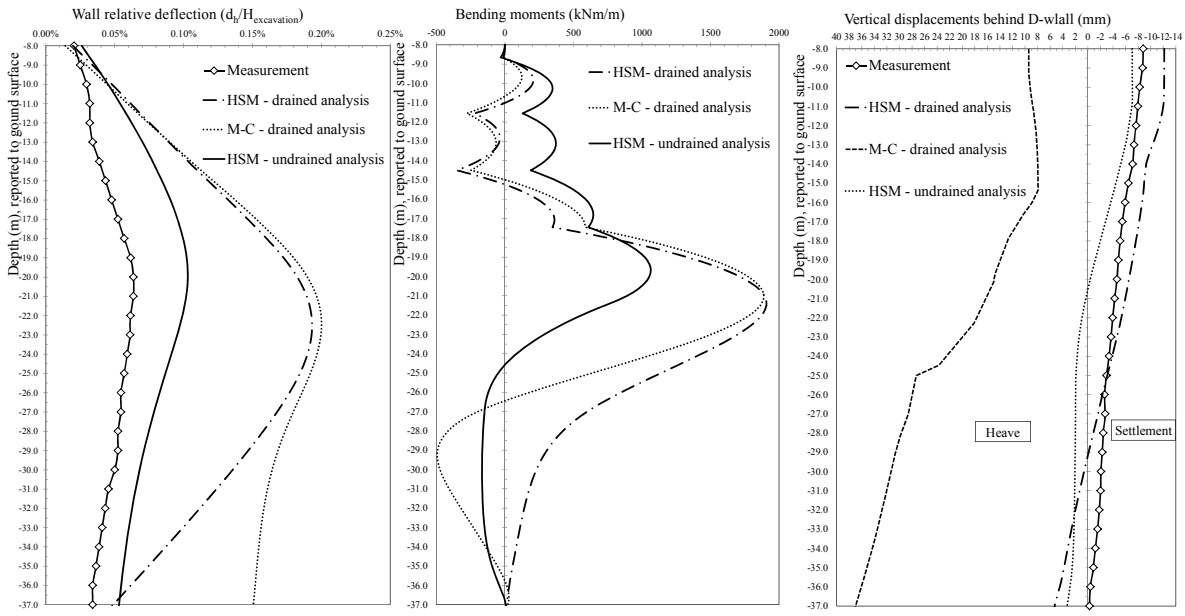

a) Relative lateral wall deflections

b) Bending moments diagram in diaphragm wall

c) Vertical displacements behind the retaining wall

Figure 7.24 Comparison of results for different types of analysis (drained vs. undrained)

To model the undrained behaviour for the current project we chose method A. It should be mentioned here, that in the current analysis only the behaviour of the Silt layer was modelled as undrained and that the analysis was provided with a consolidation stage at the end. The comparative results are presented in Figure 7.24

7.2. Case-study UNIPA (Bucharest)

7.2.1 Project Description

This case study is represented by the excavation required for an underground car parking in Bucharest, Romania. The project site is located near the city centre, on Blvd. Regina Elisabeta.

Close to the excavation site, buildings with a height of 2UG+EG+5OG (Blvd. Regina Elisabeta 3-5), UG +EG+4OG (Blvd. Regina Elisabeta 5-7), UG +EG+2OG (Blvd. Regina Elisabeta 9) can be found. These are illustrated in Figure 7.26.

The car parking area is developed on three underground levels. The three basements have an average height of 3.15m and the depth of the excavation is 11.35m. It has a length of about 150m and a maximum width of approximately 49m, with a building area of approximately 4400m^2.

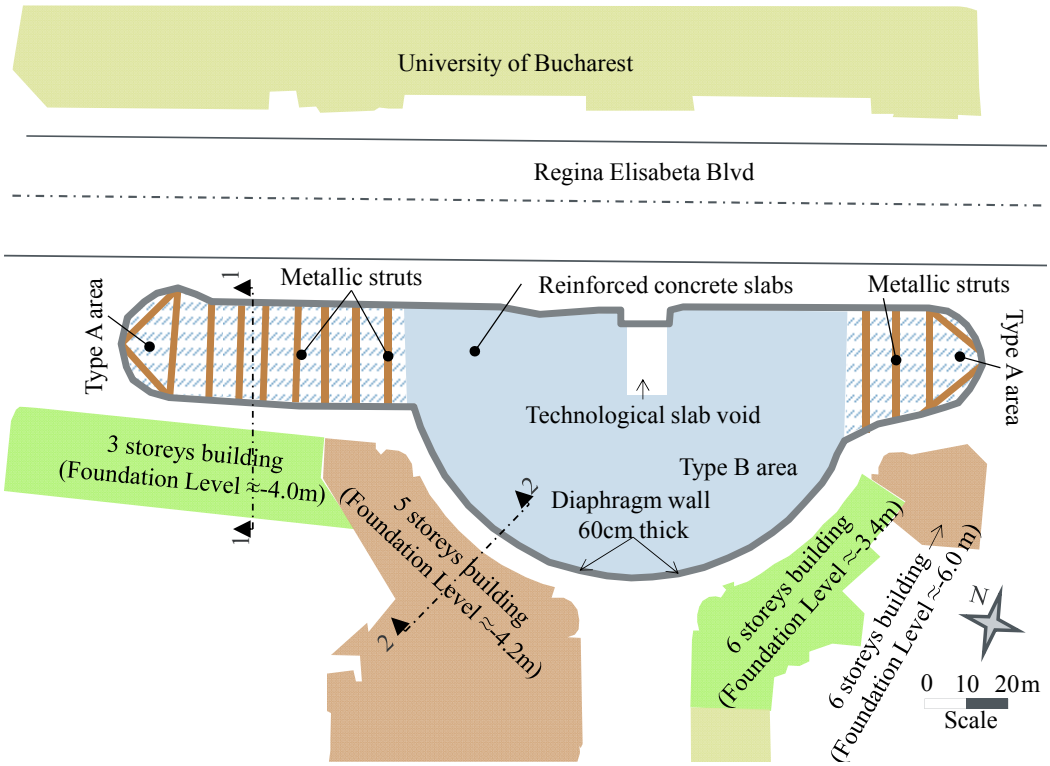

Figure 7.26 Location of the UNIPA excavation site

As shown in Figure 7.26, the complexity of the project is increased by the in-plane geometric form and the parking location (with reduced distances in relation to the surrounding historic buildings). The structure of the underground parking consists in concrete floor slab (with a thickness of 35÷45cm) supported by concrete columns with rigid reinforcement and by the embedded retaining walls, on the contour. The foundation system consists of a raft on piles (with a thickness of 90cm).

Due to the fact that, the foundation depth is located below the groundwater level, it requires dewatering works for a dry execution of the underground parking. However, for meet-

ing the waterproofing conditions, the retaining wall consisted in a diaphragm wall with waterproof joint elements. The diaphragm wall's thickness is 60cm and it was determined upon so that it satisfies the strength and deformability requirements. The depth of the diaphragm wall is about 23m from ground surface, as depicted by Figure 7.26.

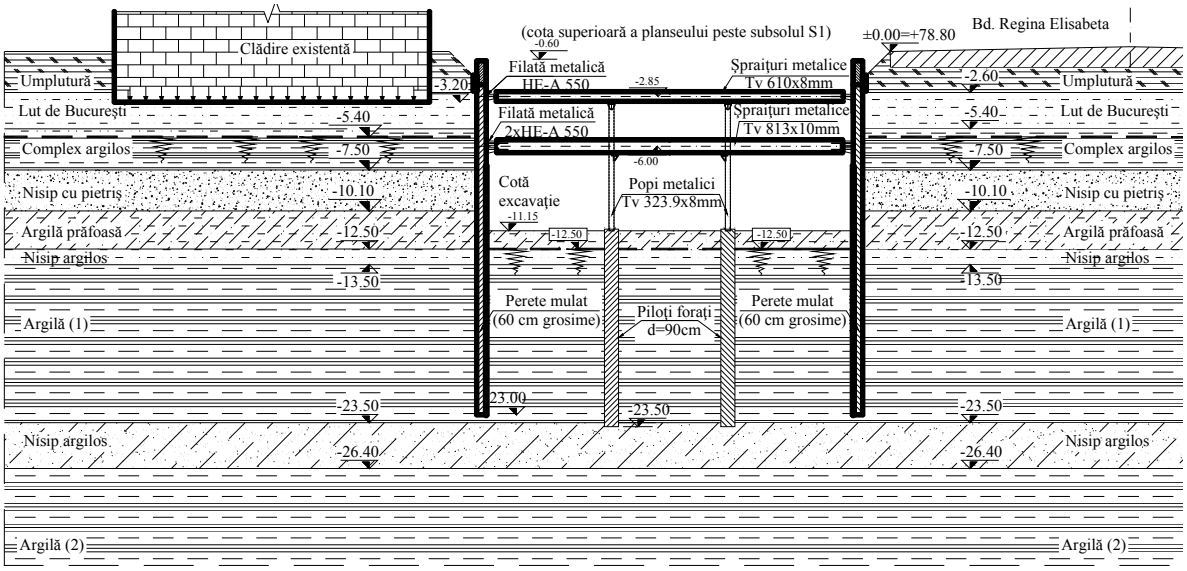

Figure 7.27 Typical cross-section for type A areas
(in final excavation construction stage: -11.15m)

The retaining wall was supported by a mixed system(Figure 7.26), which is described hereinafter. For type A areas (Figure 7.26) the supporting system consisted in two levels of struts, as shown in Figure 7.27. Both strutting level were made of metallic pipes, placed at maximum span of 6m, and they were supported vertically by H steel profiles embedded in bored piles. Due to the large in-plane expansion of area B, its supporting system consisted in concrete slabs, erected through „top-down" method. Same as on type A areas, the reinforced concrete slabs were vertically supported by H steel profiles embedded in bored piles.

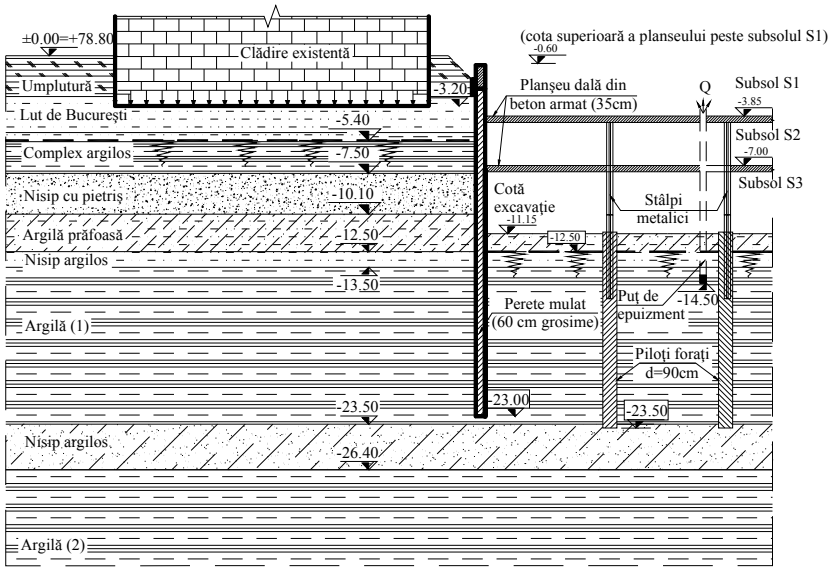

Figure 7.27 Typical cross-section for type B areas
(in final excavation construction stage: -11.15m)

Figure 7.28 illustrates a section for type B area of the supporting system. However, us-

ing the „top-down" method is justified by the level of safety that it provides. Compared to other conventional supporting systems, it's increased axial stiffness leads to lower degree level of neighbouring buildings

7.2.2 Soil stratigraphy and geotechnical parameters

The soil stratigraphy considered for the finite element analysis, was based on data revealed by the geotechnical study.

The representation of mechanical soil behaviour of is one of the most important aspects of ground-structure interaction analysis. In order to obtain proper results, the „Hardening soil" constitutive model was chosen (Schanz et al., 1999). According to the literature this model leads to more accurate results than the linear elastic-perfectly plastic Mohr-Coulomb model (Schweiger, 2008).

The distinction between primary loading and unloading is an important feature of the project in question because by the excavation process, major part of loading exhibits in the elastic domain, with a unloading/ reloading modulus (E_{ur}). The stress dependence of stiffness is considered, in the constitutive model, through an Ohde (1953) or Janbu (1961) relationship. Figure 7.29 depicts the variation of soil layers stiffness with depth, highlighting its stress dependency, in the initial phase (before the beginning of work).

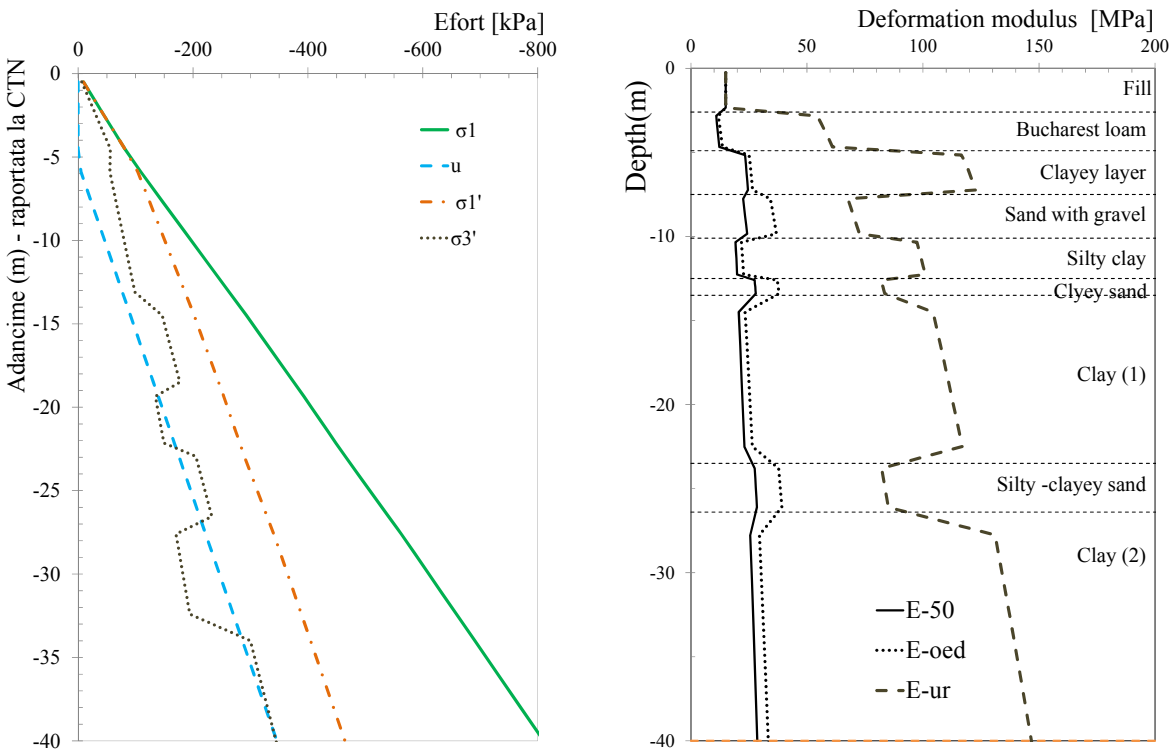

Figure 7.29 Stress dependency stiffness of soils

7.2.3 Calculation hypothesis

The analysis of the excavation induced stress and strain state was conducted by means of FEM using PLAXIS 2D software.

7.2.3.3 Construction stages

The calculations for this project consisted in a drained analysis, justified by accelerating the consolidation process due to alternating layers of non-cohesive and cohesive soil. Modelling

actual sequence of construction stages is of major importance in obtaining realistic deformations. To do this, the FEM simulation considered the construction stages described in Table 7.13.

Table 7.13: Construction stages considered in the FE simulation of UNIPA excavation

Type A area Braced excavation		Type B area top-down excavation	
No.	Construction stage	No.	Construction stage
1	Initial phase (k_0 procedure: $\sigma'_v=\gamma \times h$; $\sigma'_h=k_0 \times \sigma'_v$);	1	Initial phase (k_0 procedure: $\sigma'_v=\gamma \times h$; $\sigma'_h=k_0 \times \sigma'_v$);
2	Simulation of neighbouring buildings	2	Simulation of neighbouring buildings
3	Excavation down to -2.3m;	3	Excavation down to -2.3m;
4	Diaphragm wall execution;	4	Diaphragm wall execution;
5	Excavation down to -3.85m;	5	Excavation down to -4.20m;
6	Installation of 1st strutting level at -2.85m and groundwater lowering inside the excavation pit down to -8.50m;	6	Slab execution at level -3.85m and groundwater lowering inside the excavation pit down to -8.50m;
7	Excavation down to -6.50m;	7	Excavation down to -7.50m;
8	Installation of 2nd strutting level at -6.00m and groundwater lowering inside the excavation pit down to -12.50m;	8	Slab execution at level -7.00m and groundwater lowering inside the excavation pit down to -8.50m;
9	Excavation down to (-11.15m);	9	Excavation down to (-11.15m);

7.2.4 Results of the numerical analysis

The results presented hereinafter were obtained for the construction stage represented by the excavation down to the final level (-11.15m) – i.e. phase no. 9 in table 7.13.

To remove any doubt on the effectiveness of a plane strain analysis there has been also conducted a 3D finite element analysis. It was designed to confirm the assumptions adopted in the plane strain calculations and to make a comparative basis for displacements calculated in 2D and inclinometers measurements. The 3D FE model is shown in Figure 8. It should be noted that for the 3D-modelling of the problem, there were considered the same characteristics of geotechnical and structural parameters used in the analysis of 2D plane strain.

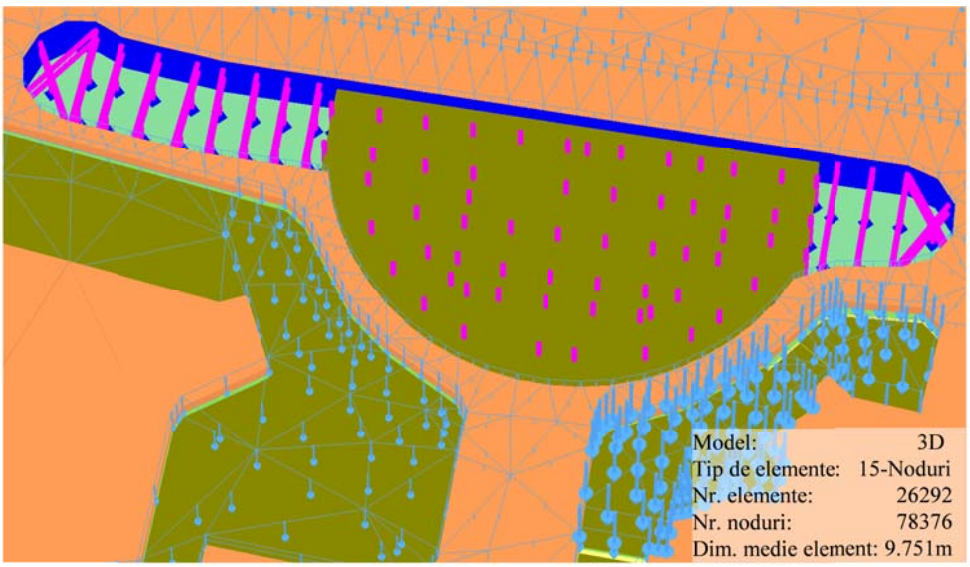

Figure 7.30 3D FE model for the UNIPA case study

In Figure 7.30 are comparatively presented the lateral deflections of the retaining wall for the two typical sections described above.

The horizontal displacement profiles calculated both 2D and 3D indicate a horizontal movement, towards the excavation, of the base of the wall (for both are types A and B), aspect which was invalidated by inclinometers measurements. However, it is believed that in reality, the wall toe has recorded yet a horizontal displacement (towards the excavation).

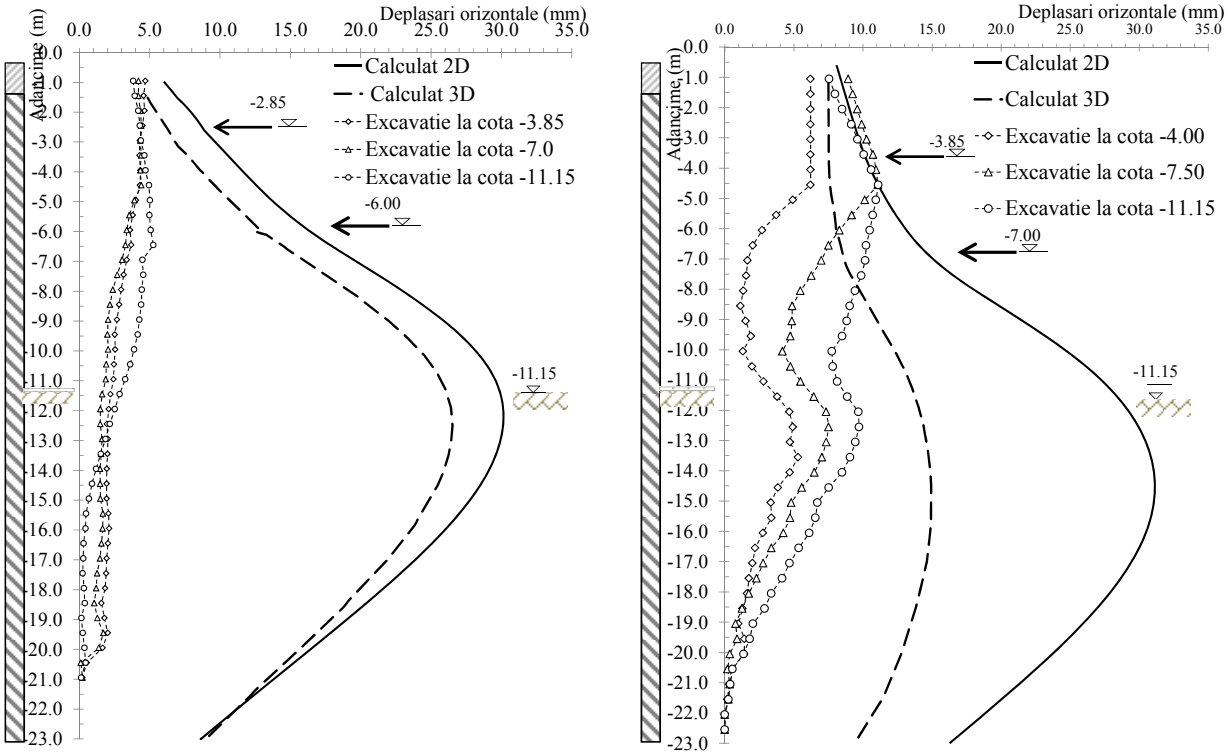

a) Diagrama deplasărilor orizontale ale peretelui de susținere pentru zona A

b) Diagrama deplasărilor orizontale ale peretelui de susținere pentru zona B

Figure 7.31: Lateral wall deflection diagrams for the two typical supporting systems of the UNIPA excavation

This shifting cannot be deduced from current measurements, because the base of the inclinometer tubes were positioned in some diaphragm wall panels at the same depth with the wall toe, while others (due to execution errors) above it (see Figure 7.31, a – where the inclinometers' base stops 2m above the wall toe). However, inclinometers measurements are based on the assumption that the value of the displacement at the basis of the inclinometer tube is zero and the values of other displacements are calculated based on this value. Thus, it justifies the almost double values of the measured diaphragm wall lateral deflections (compared to the calculated ones) for the type A area (Figure 7.31, a).

The analysis of horizontal displacement diagrams shown in Figure 7.31, b confirms that, in this case, a 2D model is conservative and realistic results are obtained through a 3D modelling. However, finite element analysis results in larger lateral displacement of the retaining wall. This can be put on the conservative estimates of geotechnical parameters of the soil layers. Another cause of this discrepancy might be the high disturbance of the in situ soil samples (which were used for the laboratory tests), resulting in low soil strength values and especially in low stiffness parameters values

Another aspect contributing probably to overestimation of the retaining wall lateral de-

flections is that the present calculations did not account for the small strain stiffness of soils, which is not the interest of the current study.

Figure 7.32 presents the normalized settlements profile behind the retaining wall, in the area defined by the primary influence zone (PIZ), as defined in section 5.2.4. From this figure, one can observe that the method proposed by Ou and Hsieh (2011) provides a good estimation of the primary influence zone as well for the excavation induced settlements profile. The only noticeable difference between the current case study and settlements envelope proposed by Ou & Hsieh is the location of the maximum settlement, i.e. for the current case study it occurs at a distance of 0.28ZIP.

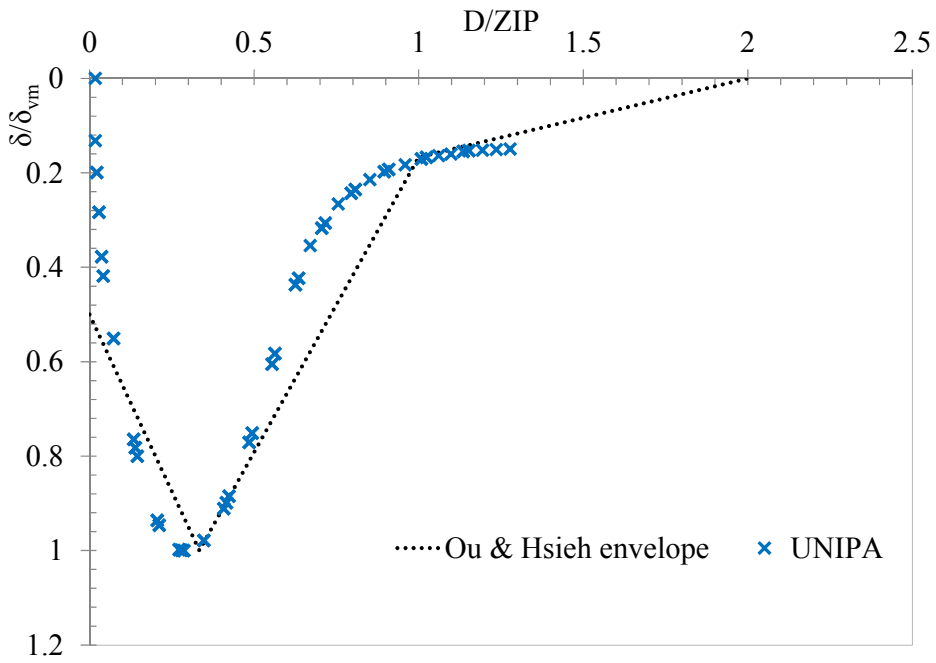

Figure 7.32: Greenfield normalized settlements behind the retaining wall for type B area

8. Conclusions and personal contributions

8.1 Conclusions

This chapter reviews the main accomplishments of the thesis as well as the possible future lines of research.

In order to reduce the risk of failure (ultimate limit state) of deep excavations and that of damaging neighbouring buildings (serviceability limit state), the design of retaining works should be done by thoroughly analysing the induced deformations and checked by a few simple empirical and analytical methods (some of which are presented in chapter 2 and 5). Thus, a deep understanding of the deformation mechanism is required as well as knowledge regarding the transfer mechanism of stresses within soil mass.

The present thesis analyses the issue of estimating the soil displacements around deep excavations. Firstly, the influence of the features of neighbouring buildings is analysed using a parametric study on a characteristic model whose dimensions are statistically established based on an analysis of an updated database regarding the retaining walls and the excavation –induced displacements. Secondly, this aspect is researched based on some deep excavations case studies (with depths greater than 10m). The main objective of the research is the analysis

of the excavation-induced ground movements.

The performance of deep excavations is influenced by various factors, the most important of them being: the depth of the excavation, the type and the bending stiffness of the retaining wall, the support system configuration and the vertical distance between strutting levels, soil layers and their geotechnical parameters, groundwater level, the weight of the neighbouring buildings, the distance between these and the limits of excavation, the geometry of excavation and last but not least the workmanship. In order to prevent the uncertainties related to these factors, the current practice in the field has developed a variety of methods which envisage the adoption of some safety factors within the calculation (see chapter 2). This calculation approach provides a guarantee for the reliability of the retaining works. On the other hand, the excavation project must also meet the corresponding requirements regarding the deformations induced by neighbouring buildings.

8.2 Personal contributions

This section presents the issues regarding the novelty of the research that have not been presented elsewhere in the literature. The aspects will be addressed chronologically as they appear in the thesis.

The first contribution refers to a synthesis of both Romanian and international standards regarding the calculation of retaining works and the methods for applying safety factors. This comparative perspective revealed the absence of provisions regarding the estimation of the influence zone of deep excavations (most of them in densely built areas). Thus, I did a synthesis of methods used to estimate the influence zone of excavations. Based on the analysis of the existing methods presented by the literature in the field, I emphasized the extension of the influence zone beyond the limits of the excavation. Furthermore, I also presented the existing methods for determining the magnitude of excavation-induced displacements.

Moving onwards, the thesis presents a review of various criteria for assessing the damage of buildings subjected to excavation-induced ground movements. This aspect is particularly important since it is a sine qua non condition for estimating the influence of excavations on neighbouring buildings and to decide upon the necessary measures to minimize this influence until its cancellation.

The forth contribution refers to extending an existing 296 case-studies database on retaining walls and ground movements due to deep excavations by adding 27 more case studies, some of them from the literature in the field and others from the ones presented in chapter 7.

Perhaps the most important contribution refers to the proposed excavation influence index. Thus, an excavation-neighbouring building systemic analysis was conducted through a parametric study with the purpose of emphasizing the factors that influence the performance of excavations but also their effects on the neighbouring buildings. The result of such an analysis was an excavation influence index, through which the magnitude of vertical displacements induced behind the retaining wall may be expressed based on the lateral wall deflection.

Furthermore, a nonlinear numerical analysis using the finite element method on three case-studies of deep excavations in urban areas was elaborated. Based on this analysis, some recommendations were issued regarding the improvements of the results of monitoring the lateral displacements of retaining walls.

Last but not least, recommendations were issued regarding updating the current national norms for designing of deep excavations in densely built areas. The recommendations refer to

including some methods for quantitatively estimating the influence zone of excavations (expansion and magnitude) as well as criteria for evaluating the damages produced by building situated in this area.

8.3 Future lines of research

- elaborating some studies regarding the analysis of factors that influence the displacements induced by excavations and the measures necessary to reduce their intensity;
- calibration of the current calculation methods for deep excavations, including insitu measurements of excavation-induced displacements in the Romanian soils;

Selected references

Adam, D., Kopf, F., Paulmichl, I., (2010) *Modelling and Simulation of Heavy Tamping Dynamic Response of the Ground*, Proceedings of the 14th DECGE 2010, Bratislava, Slovacia

Alphan, I. (1967), *The empirical evaluation of the coefficient K_0 and K_{0r}*, ASCE Soils and Foundations, vol. 7, pp 31–40.

Bakker, K.J., (2005), *A 3D FE Model for Excavation Analysis*, 5th Geotechnical Aspects of Underground Construction in Soft Ground, pp. 473-478.

Bolton, M.D, (1996), *Geotechnical design of retaining walls*, The Structural Engineering, vol. 74, no. 21, pp 365-369.

Boone, S.J, (2001). *Assessing construction and settlement-induced building damage: a return to fundamental principles*, Proceedings, Underground Constructions, Institution of Mining and Metalurgy, London, pp 559-570.

Boscardin, M.D., Cording, E.J. (1989), *Building Response to Excavation-Induced Settlement*, Journal of Geotechnical Engineering, ASCE, Vol. 115, No.1, pp 1-21.

Boți N, Stanciu, A., Lungu, I., Croitoru, D., (2008), *Refacerea rampelor de acces la poduri afectate de inundații*, Lucrările celei de a XI-a conferință națională de geotehnică și fundații, Timișoara, România, pp 562-567.

Bowles, J. E. (1996), *Foundation Analysis and Design*, Ediția a 5-a., McGraw-Hill Book Company, New York.

Burland, J.B., Wroth, C.P, (1975), *Settlement of Buildings and Associated Damage*, Building Research Establishment Current Paper, Building Research Establishment, Watford.

Gudehus, G., Weißenbach, A., (1995), *Limit state design of structural parts at and in the ground*, Ground Engineering 29, No. 7, pp 42 - 45

Hsieh, P.G., Ou, C. Y. (1998), *Shape of ground surface settlement profiles caused by excavation*, Canadian Geotechnical Journal, vol. 35, nr. 6, pp 1004–1017

Long, M., (2001), *Database for Retaining Wall and Ground Movements due to Deep Excavations*, Journal of Geotechnical and Geonvironmental Engineering, vol. 127, nr. 3, pp 203-224.

Ou, C.-Y., Chiou, D.C., Wu, T.S. (1996), *Three-dimensional finite element analysis of deep excavations*, Journal of Geotechnical and Geoenvironmental Engineering, ASCE, Vol.122, ediția 5, pp 337−345.

Peck, R.B., (1969), *Deep Excavations and Tunneling in Soft Ground*, Proceedings of the 7th International Conference on Soil Mechanics and Foundation Engineering, pp 225–281.

Potts, D.M., Addenbrooke T.I., (1997) *A structure's influence on tunnelling induced ground movements*, Proceedings of the ICE – Geotechnical Engineering, vol. 125, nr. 3, pp 109–125.

Potts, D.M, Zdravkovic, L., (2001), Finite Element Analysis in Geotechnical Engineering: Theory, Thomas Telford.

Saidel, T., Căpraru, C., Marcu, A., (2010), *Influence of constitutive laws and geotechnical parameters on deep excavations design, and evaluation of their influence on neighbouring buildings: examples from recent projects in Bucharest*, Proceedings of the 14th DECGE 2010, Bratislava, Slovacia.

Tschuchnigg F., Schweiger H. F., Fröhlich K., (2010) *3D Finite Element analysis of a deep foundation with diaphragm wall panels*, Geotechnical challenges in megacities, Russia.

Wehnert, M., (2006), Ein Beitrag zur dranierten und undränierten Analyse in der Geotechnik, PhD thesis, TU Stuttgart, Germany.